Time-Harmonic Line-Force Acting on the Surface of a Semi-Infinite Elastic Half-Space.

University of Liverpool,
Thesis for M.Math (MATH499),
Finley Boulton.

1 Introduction.

Much of the original work on this problem was considered by Lamb [1904] with his motivation being that of the phenomena of earthquakes in seismology, and the collision of elastic solids. He considers a time-harmonic point surface source, and a time-harmonic line surface source, both with normal loading. First he considers the problem in 2-dimensions then generalises it to 3-dimensions. He obtains solutions only for surface waves, but briefly touches on how to possibly obtain interior displacements as well as buried sources.

Using what Lamb [1904] suggests on buried sources Nakano [1925] analyses how Rayleigh waves form and propagate under the circumstances of a buried source, exclusively in 2-dimensions. He obtains approximate expressions for the free surface waves using the method of steepest descent. Noting that he finds there is no surface waves to be found directly above the source, but instead they manifest at some distance away from the source. However, there were inconsistencies in his results when he replaces a time-harmonic source with a general pulse of arbitrary form.

Jeffreys [1926] Discuses a problem which arose in studies of seismology where observed and predicted data differ, and ordinary laws of refraction break down at short distances. The problem is to resolve disturbances created by a spherical explosion in the upper of two superposed layers, where the bottom layer has different material parameters such that pressure waves are transmitted with greater velocity than the upper. He finds such disturbances in the form of an infinite series of pulses each of which are expressed with a contour integral using the Bromwich expansion method. He finds that this explosion creates disturbances on the surfaces involving the expected direct and reflected waves, but there is also a refracted finite amplitude wave. This model was in reasonable accordance with observed data. However, he considers a simplified model neglecting rigidity and curvature.

Muskat [1933] Considers the problem of reflection and refraction of incoming waves at the interface of two linearly elastic solids. He finds solutions in the form of pulses being received at a given point.

Later Lapwood [1949] considers a cylindrical pulse emitted from a line source buried in a semi-infinite elastic solid. He gives the exact solution in terms of double integrals which are approximated for when the depth of the source point and reception point are small relative to their distance. He does this in order to describe the nature in which various pulses arrive at this reception point, with the aim to shed light on seismological problems.

The problem in Lapwood [1949] is elaborated on in Newlands [1952] where she investigates the same cylindrical pulse emitted from a line source, but this time the source is buried a surface layer of an elastic solid which is overlying a semi-infinite elastic solid of differing material parameters. Again the exact solution is written in terms of double integrals which are subsequently approximated to get a pulse representation.

Heelan [1953b] and Heelan [1953a] present interesting problems of a buried cylindrical source of finite length, the walls of which are subjected to symmetric normal and tangential stresses in an elastic medium and a layered elastic medium respectively. In these two papers he tries to reproduce, in mathematical form, the disturbance generated by the detonation of a charge in a cylindrical shot hole and hopes that information gathered about the divergent wave system may be of use in seismic prospecting. In particular he notes that no attempt had been made up to that point to use beamed shear waves, as it was thought artificial disturbances generated little shear energy. He solves both problems using an asymptotic method in the far field (the method of steepest descent). Heelan [1953a] makes use of a very similar approach to get approximate solutions for the case of a discontinuous layered medium.

Miller and Pursey [1954] examine 4 different problems: (a) an infinitely long strip of finite width vibrating normally with respect to the surface; (b) the same as (a) but with tangential vibrations with respect to the surface; (c) a circular disk vibrating of finite radius vibrating normally to the surface; (d) a torsional source in the form of a circular disk of finite radius undergoing rotational oscillations about its centre. They find the exact results again in terms of definite integrals which require approximation. The cases (a) and (b) are asymptotically approximated in the far field in a similar manner to how we will solve the problem presented in this dissertation. The case of surface waves is also considered for (a) and (b). The cases (c) and (d) are also asymptotically approximated in the far field but the calculation is done in a slightly different manner, making use of the Bessel function (the method of steepest descent is still used). Interestingly, they find that for the case of (c) identical polar diagrams will be found to that of case (a). Surface waves are found for (c). Results for (d) are found in a similar way to (c). It is found that for the case of (d) no surface waves are produced and that angular displacement is constant over a hemispherical shell. Radiation impedance (a measure of the ease in which waves pass through a particular medium) is found for (a), (b), (c), and (d); where the numerical evaluation of the radiation impedance integral for (a) is covered in detail.

Takeuchi and Kobayashi [1955] consider wave Generations from Line Sources within the solid. They follow the problem closely to that of Nakano [1925] and Lapwood [1949]. However, they perform numerical analysis to study tremors near the source. They state that methods pertaining to the derivation of displacements corresponding to pressure, shear and Rayleigh waves need to be summed up to get the true displacement at any time. And that this summing up has not yet been performed. They find a few notable results regarding Rayleigh waves appearing at certain distances from the source and displacement near the source.

Problems of Elastic waves in layered media are covered in the book Ewing et al. [1957] with aim to unify studies on seismology, geophysical prospecting, acoustics, and electromagnetism. Naturally, a broad range of problems are covered in this text, including problems similar to the one discussed in this dissertation.

Copson [1962] is a book about asymptotic methods. Importantly it contains details on a modified version of Watson's lemma which we will use to evaluate the branch cut integrals. The book also contains methods for other definite integrals, as-well-as (but not limited to), differential equations, Bessel functions, Mathieu functions, and 3-dimensional wave problems.

Graff [1991] is another book specifically about wave motion in elastic solids, similar to Ewing et al. [1957]. The asymptotic analysis present here will follow closely from Graff [1991] [pp. 344-353]. The book as a hole contains a great wealth of knowledge, considering everything from wave motion in strings to wave propagation in plates and rods. Specifically, Graff [1991] covers other material closely related to this topic of waves in semi-infinite media, for example, waves in layered media, buried sources, tangential surface loads, etc.

Problems of waves is also covered in detail in the book Achenbach [2012]. The book covers many problems, everything from motion in a one dimensional continuum, to waves in viscoelastic solids. Achenbach [2012], Graff [1991], and Ewing et al. [1957] cover a great deal of the same information. All of which are worth looking at when considering problems of wave motion in elastic solids. Achenbach [2012] covers this same problem (and solves it in the same manner), as well as, the interesting transient load case.

Contents

In this dissertation we will consider the problem of a linearly elastic half space orientated such that the x, z-plane is the surface and the x, y-plane will be the vertical plane with $y > 0$ pointing down into the solid. The half space will be subjected to unit loading on a strip normal to the surface from $-a < x < a$ and invariant with respect to z. Hence, we have a resulting situation of plane strain. Where $u_z = \partial/\partial z = 0$. See Graff [1991] [pp. 312] for a visualisation on the geometry of the half space.

In section 2 we will derive four key results; The displacement equations, the wave equations, the stresses, and the boundary conditions. Then in section 3 we apply the Fourier transform to these results so that we can solve the system and obtain exact solutions for the displacements in terms of definite integrals. Key properties of these integrals (poles, branch points, etc.) are then found in section 4. Using this knowledge in section 5 we first neglect the contribution from the poles to obtain asymptotic approximations in the far field for interior displacements. We then plot the results of these approximations in section 6 before moving on to consideration of the special case of surface waves in section 7. In section 8 we perform a finite element analysis of the problem, and compare these numerical results to asymptotic results. Finally, In section 9, we present our concluding remarks on this dissertation.

The analysis of such problems can find application in many fields. For example one could use the similar problem of buried sources to better understand the phenomena of earthquakes in seismology, and thus design more resistant structures. Another possible use is that of oil, natural gas exploration, and other related fields of seismic prospecting. For example, one could consider a layered medium and look at the reflected waves in an attempt to predict the location of such resources for extraction. Also, in the field of engineering, one could consider the case of colliding elastic solids and the resulting waves to analyse stress and possible points of failure in various mechanical structures and devices.

2 Governing Equations.

To begin we need to derive the displacement equations of motion. This is done by considering

$$\sigma_{ij,j} + \rho F_i = \rho \ddot{u}_i, \qquad \text{(Linear Momentum Balance Law (LMBL))} \tag{2.1}$$

$$e_{ij} = \frac{1}{2}\left(u_{i,j} + u_{j,i}\right), \qquad \text{(Strain tensor)} \tag{2.2}$$

$$w_{ij} = \frac{1}{2}\left(u_{i,j} - u_{j,i}\right). \qquad \text{(Rotation tensor)} \tag{2.3}$$

Where the (LMBL) is a result from the conservation of momentum within a continuum, the strain tensor defines the relative change in the position of points within a continuum that has undergone a deformation, and the rotation tensor defines the relative change in position of points within a continuum that has undergone a rotation. Here we also have used standard index notation where repeated indices are summed. Furthermore, u_i is the displacement vector of a material point, the mass density per unit volume of the material is ρ, and F_i is the body force per unit mass of material. We also require that the stress tensor is symmetric i.e., $\sigma_{ij} = \sigma_{ji}$, which is the Angular Momentum Balance Law (AMBL). λ, μ are the Lamé elastic constants. These may be expressed with other elastic constants, such as, Young's modulus, Poisson's ratio, bulk modulus, etc.

As our solid is linearly elastic we have a linear relationship between stress and strain, and given stress is a function of strain we can write

$$\sigma_{ij} = c_{ijkl}e_{kl}. \qquad \text{(Generalised Hooke's Law)} \tag{2.4}$$

c_{ijkl} a isotropic Cartesian tensor of rank 4 of linear elastic moduli. As we assume the half space is an isotropic elastic solid; with the symmetry of σ_{ij} and e_{kl}, we have $c_{ijkl} = c_{jikl} = c_{ijlk} = c_{jilk}$. Thus we derive relation

$$\begin{aligned} c_{ijkl} &= \varepsilon_{ijr}\varepsilon_{klr}, \\ &= \lambda\delta_{ij}\delta_{kl} + \mu\delta_{ik}\delta_{jl} + \mu'\delta_{il}\delta_{jk}. \\ c_{jikl} &= \varepsilon_{jir}\varepsilon_{klr}, \\ &= \lambda\delta_{ji}\delta_{kl} + \mu\delta_{jk}\delta_{il} + \mu'\delta_{jl}\delta_{ik}. \\ &\implies \mu = \mu'. \\ \implies c_{ijkl} &= \lambda\delta_{ij}\delta_{kl} + \mu\left(\delta_{ik}\delta_{jl} + \delta_{il}\delta_{jk}\right). \end{aligned} \tag{2.5}$$

Where λ, μ are the Lamé elastic constants, and ε is the alternating tensor. Hence we get the equation for Cauchy's stress tensor

$$\begin{aligned} \sigma_{ij} &= c_{ijkl}e_{kl}, \\ &= \lambda\delta_{ij}\delta_{kl}e_{kl} + \mu\left(\delta_{ik}\delta_{jl} + \delta_{il}\delta_{jk}\right)e_{kl}, \\ &= \lambda\delta_{ij}e_{kk} + 2\mu e_{ij}. \end{aligned} \tag{2.6}$$

Noting that e_{kk} is the trace of the strain tensor and the dilation of the material. Now we are in a position to substitute in (2.2) (Strain tensor) to obtain Cauchy's stress tensor (2.6) in terms of displacement.

$$\sigma_{ij} = \lambda\delta_{ij}u_{k,k} + \mu\left(u_{i,j} + u_{j,i}\right). \tag{2.7}$$

And now by substituting (2.4) (Generalised Hooke's Law) into (2.1) (LMBL) we get the displacement equations of motion

$$\begin{aligned} &\lambda u_{k,ki} + \mu\left(u_{i,jj} + u_{j,ij}\right) + \rho F_i = \rho\ddot{u}_i \iff \\ \iff &\mu u_{i,jj} + (\lambda + \mu)\,u_{k,ki} + \rho F_i = \rho\ddot{u}_i. \end{aligned} \tag{2.8}$$

Or in vector form

$$\mu\nabla^2\mathbf{u} + (\lambda + \mu)\nabla\left(\nabla\cdot\mathbf{u}\right) + \rho\mathbf{F} = \rho\ddot{\mathbf{u}}. \tag{2.9}$$

Where ∇^2 is Laplace's operator, and remembering that derivatives with respect to z vanish. An expression for $\nabla^2\mathbf{u}$ can be obtained by the identity

$$\begin{aligned} &\nabla\times\left(\nabla\times\mathbf{u}\right) = \nabla\left(\nabla\cdot\mathbf{u}\right) - \nabla^2\mathbf{u} \\ &\implies \nabla^2\mathbf{u} = \nabla\left(\nabla\cdot\mathbf{u}\right) - \nabla\times\left(\nabla\times\mathbf{u}\right), \end{aligned} \tag{2.10}$$

where the preceding can be proven utilising index notation. Substituting in (2.10) into (2.9) to arrive at

$$(\lambda + 2\mu)\,\nabla\left(\nabla\cdot\mathbf{u}\right) - \mu\nabla\times\left(\nabla\times\mathbf{u}\right) + \rho\mathbf{F} = \rho\ddot{\mathbf{u}}. \tag{2.11}$$

e_{kk}, the trace of the strain tensor (the dilation), for conditions of plain strain can be written by

$$\begin{aligned} e_{kk} &= \frac{1}{2}\left(\frac{\partial u_k}{\partial x_k} + \frac{\partial u_k}{\partial x_k}\right) = \frac{\partial u_k}{\partial x_k}, \\ &= \frac{\partial u_x}{\partial x} + \frac{\partial u_y}{\partial y} + \cancelto{0}{\frac{\partial u_z}{\partial z}}, \\ &= \frac{\partial u_x}{\partial x} + \frac{\partial u_y}{\partial y}, \\ &= \nabla\cdot\mathbf{u} = \Delta. \end{aligned} \tag{2.12}$$

We also have the rigid rotation

$$
\begin{aligned}
W = \nabla \times \mathbf{u} = \nabla \times (u_x, u_y, 0) = \left(0, 0, \frac{\partial u_x}{\partial y} - \frac{\partial u_x}{\partial y}\right),\\
\implies W\mathbf{k} = \left(\frac{\partial u_x}{\partial y} - \frac{\partial u_x}{\partial y}\right)\mathbf{k}.
\end{aligned} \tag{2.13}
$$

We have time-harmonic line loading $e^{i\omega t}$, thus

$$
u_x(x, y, t) = u_x(x, y)e^{i\omega t}, \quad u_y(x, y, t) = u_y(x, y)e^{i\omega t} \tag{2.14}
$$

Then substituting the derivatives of (2.14), and (2.13), (2.12) into (2.11). The vector displacement equation of motion (2.11) may be written as

$$
(\lambda + 2\mu)\nabla\Delta - \mu\nabla \times W = \rho\ddot{\mathbf{u}}. \tag{2.15}
$$

Or

$$
(\lambda + 2\mu)\frac{\partial \Delta}{\partial x} + \mu\frac{\partial W}{\partial y} + \rho\omega^2 u_x = 0, \tag{2.16}
$$

$$
(\lambda + 2\mu)\frac{\partial \Delta}{\partial y} - \mu\frac{\partial W}{\partial x} + \rho\omega^2 u_y = 0. \tag{2.17}
$$

From here we eliminate W and Δ successively to obtain the wave equations. Starting with Δ we take the partial derivative with respect to x of (2.16) then add this to the partial derivative with respect to y of (2.17) (or in shorthand $\partial/\partial x$(2.16) + $\partial/\partial y$(2.17))

$$
\begin{aligned}
(\lambda + 2\mu)\frac{\partial^2 \Delta}{\partial x^2} + \cancel{\mu\frac{\partial^2 W}{\partial y \partial x}} + \rho\omega^2\frac{\partial u_x}{\partial x} + (\lambda + 2\mu)\frac{\partial^2 \Delta}{\partial y^2} - \cancel{\mu\frac{\partial^2 W}{\partial x \partial y}} + \rho\omega^2\frac{\partial u_y}{\partial y} = 0,\\
(\lambda + 2\mu)\nabla^2\Delta + (\rho\omega^2)\left(\frac{\partial u_x}{\partial x} + \frac{\partial u_y}{\partial y}\right) = 0,\\
\nabla^2\Delta + \frac{\rho\omega^2}{(\lambda + 2\mu)}\Delta = 0,\\
\nabla^2\Delta + c_1^2\omega^2\Delta = 0,\\
\nabla^2\Delta + k_1^2\Delta = 0.
\end{aligned} \tag{2.18}
$$

Now for W we take the partial derivative with respect to y of (2.16) then minus the partial derivative with respect to x of (2.17) (or in shorthand $\partial/\partial y$(2.16) - $\partial/\partial x$(2.17))

$$
\begin{aligned}
\cancel{(\lambda + 2\mu)\frac{\partial^2 \Delta}{\partial x \partial y}} + \mu\frac{\partial^2 W}{\partial y^2} + \rho\omega^2\frac{\partial u_x}{\partial y} - \cancel{(\lambda + 2\mu)\frac{\partial^2 \Delta}{\partial y \partial x}} + \mu\frac{\partial W}{\partial x^2} - \rho\omega^2\frac{\partial u_y}{\partial x} = 0,\\
\mu\nabla^2 W + \rho\omega^2\left(\frac{\partial u_x}{\partial y} - \frac{\partial u_x}{\partial y}\right) = 0,\\
\nabla^2 W + \frac{\rho\omega^2}{\mu}W = 0,\\
\nabla^2 W + c_2^2\omega^2 W = 0,\\
\nabla^2 W + k_2^2 W = 0.
\end{aligned} \tag{2.19}
$$

With

$$
\nabla^2 = \frac{\partial^2}{\partial x^2} + \frac{\partial^2}{\partial y^2}, \quad c_1^2 = \frac{\rho}{(\lambda + 2\mu)}, \quad k_1^2 = c_1^2\omega^2, \tag{2.20}
$$

$$c_2^2 = \frac{\rho}{\mu}, \quad k_2^2 = c_2^2\omega^2. \tag{2.21}$$

Using (2.2) (strain tensor) and (2.6) (Cauchy stress tensor), we directly find the stresses

$$\sigma_{yy} = \lambda\Delta + 2\mu\frac{\partial u_y}{\partial y}, \tag{2.22}$$

$$\sigma_{xy} = \mu\left(\frac{\partial u_x}{\partial y} + \frac{\partial u_y}{\partial x}\right), \tag{2.23}$$

$$\sigma_{yz} = 0. \tag{2.24}$$

To Express σ_{yy} in terms of Δ, W, we take the partial derivative with respect to y of (2.17), then the partial derivative with respect to x of (2.16) (or in shorthand $\partial/\partial y(2.17)$ and then $\partial/\partial x(2.16)$)

$$\begin{aligned}
\frac{\partial}{\partial y}(1.17):\quad & (\lambda+2\mu)\frac{\partial^2\Delta}{\partial y^2} - \mu\frac{\partial^2 W}{\partial x\partial y} + \rho\omega^2\frac{\partial u_y}{\partial y} = 0,\\
\implies\quad & \frac{\partial u_y}{\partial y} = \frac{1}{\rho\omega^2}\left[\mu\frac{\partial^2 W}{\partial x\partial y} - (\lambda+2\mu)\frac{\partial^2\Delta}{\partial y^2}\right],
\end{aligned} \tag{2.25}$$

$$\begin{aligned}
\frac{\partial}{\partial x}(1.16):\quad & (\lambda+2\mu)\frac{\partial^2\Delta}{\partial x\partial y} + \mu\frac{\partial^2 W}{\partial y^2} + \rho\omega^2\frac{\partial u_x}{\partial y} = 0,\\
\implies\quad & \frac{\partial u_x}{\partial x} = \frac{1}{\rho\omega^2}\left[-\mu\frac{\partial^2 W}{\partial x\partial y} - (\lambda+2\mu)\frac{\partial^2\Delta}{\partial x^2}\right].
\end{aligned} \tag{2.26}$$

Now substitute (2.25), (2.26) into (2.22) and rearrange

$$\begin{aligned}
\sigma_{yy} &= \lambda\Delta + 2\mu\frac{\partial u_y}{\partial y} = \lambda\left(\frac{\partial u_x}{\partial x} + \frac{\partial u_y}{\partial y}\right) + 2\mu\frac{\partial u_y}{\partial y},\\
&= \frac{\lambda}{\rho\omega^2}\left[-\mu\frac{\partial^2 W}{\partial x\partial y} - (\lambda+2\mu)\frac{\partial^2\Delta}{\partial x^2} + \mu\frac{\partial^2 W}{\partial x\partial y} - (\lambda+2\mu)\frac{\partial^2\Delta}{\partial y^2}\right] + \frac{2\mu}{\rho\omega^2}\left[\mu\frac{\partial^2 W}{\partial x\partial y} - (\lambda+2\mu)\frac{\partial^2\Delta}{\partial y^2}\right],\\
&= -\frac{\lambda(\lambda+2\mu)}{\rho\omega^2}\left(\frac{\partial^2\Delta}{\partial x^2} + \frac{\partial^2\Delta}{\partial y^2}\right) + \frac{2\mu}{\rho\omega^2}\left[\mu\frac{\partial^2 W}{\partial x\partial y} - (\lambda+2\mu)\frac{\partial^2\Delta}{\partial y^2}\right],\\
&= \frac{2\mu}{\rho\omega^2}\left[2\frac{\partial^2 W}{\partial x\partial y}\right] - \frac{\lambda(\lambda+2\mu)}{\rho\omega^2}\frac{\partial^2\Delta}{\partial y^2} - \frac{2\mu(\lambda+2\mu)}{\rho\omega^2}\frac{\partial^2\Delta}{\partial y^2} - \frac{\lambda(\lambda+2\mu)}{\rho\omega^2}\frac{\partial^2\Delta}{\partial x^2},\\
&= \frac{2\mu}{\rho\omega^2}\left[2\frac{\partial^2 W}{\partial x\partial y}\right] - \frac{\partial^2\Delta}{\partial y^2}\left(\frac{\lambda(\lambda+2\mu)}{\rho\omega^2} + \frac{2\mu(\lambda+2\mu)}{\rho\omega^2}\right) - \frac{\lambda(\lambda+2\mu)}{\rho\omega^2}\frac{\partial^2\Delta}{\partial x^2},\\
&= \frac{2\mu}{\rho\omega^2}\left[2\frac{\partial^2 W}{\partial x\partial y}\right] - \frac{\partial^2\Delta}{\partial y^2}\left(\frac{\lambda^2 + 4\mu\lambda + 4\mu^2}{\rho\omega^2}\right) - \frac{\lambda(\lambda+2\mu)}{\rho\omega^2}\frac{\partial^2\Delta}{\partial x^2},\\
&= \frac{2\mu}{\rho\omega^2}\left[2\frac{\partial^2 W}{\partial x\partial y}\right] - \frac{(\lambda+2\mu)^2}{\rho\omega^2}\frac{\partial^2\Delta}{\partial y^2} - \frac{\lambda^2 + 2\mu\lambda}{\rho\omega^2}\frac{\partial^2\Delta}{\partial x^2},\\
&= \frac{\mu^2}{\rho\omega^2}\left[2\frac{\partial^2 W}{\partial x\partial y} - \frac{(\lambda+2\mu)^2}{\mu^2}\frac{\partial^2\Delta}{\partial y^2} - \frac{\lambda^2 + 2\mu\lambda}{\mu^2}\frac{\partial^2\Delta}{\partial x^2}\right],\\
&= \frac{\mu^2}{\rho\omega^2}\left[2\frac{\partial^2 W}{\partial x\partial y} - k^4\frac{\partial^2\Delta}{\partial y^2} - \frac{\mu\lambda^2 + 2\mu^2\lambda}{\mu^3}\frac{\partial^2\Delta}{\partial x^2}\right],\\
&= \frac{\mu^2}{\rho\omega^2}\left[2\frac{\partial^2 W}{\partial x\partial y} - k^4\frac{\partial^2\Delta}{\partial y^2} - \frac{\mu\lambda^2 + 4\mu^2\lambda + 4\mu^3 - 2\mu^2\lambda - 4\mu^2}{\mu^3}\frac{\partial^2\Delta}{\partial x^2}\right],
\end{aligned}$$

$$
\begin{aligned}
=&\frac{\mu^2}{\rho\omega^2}\left[2\frac{\partial^2 W}{\partial x \partial y} - k^4\frac{\partial^2\Delta}{\partial y^2} - \frac{\mu(\lambda^2+4\mu\lambda+4\mu^2)-2\mu^2\lambda-4\mu^2}{\mu^3}\frac{\partial^2\Delta}{\partial x^2}\right],\\
=&\frac{\mu^2}{\rho\omega^2}\left[2\frac{\partial^2 W}{\partial x \partial y} - k^4\frac{\partial^2\Delta}{\partial y^2} - \left(\frac{(\lambda+2\mu)^2}{\mu^2} - 2\frac{\lambda+2\mu}{\mu}\right)\frac{\partial^2\Delta}{\partial x^2}\right],\\
\sigma_{yy} =&\frac{\mu^2}{\rho\omega^2}\left[2\frac{\partial^2 W}{\partial x \partial y} - k^4\frac{\partial^2\Delta}{\partial y^2} - k^2\left(k^2-2\right)\frac{\partial^2\Delta}{\partial x^2}\right]. \qquad (2.27)
\end{aligned}
$$

Where $k^2 = (\lambda+2\mu)/\mu = k_2^2/k_1^2$. And now for σ_{xy} we do nearly the same procedure by taking the partial derivative with respect to y of (2.16) and then the partial derivative with respect to x of (2.17) (or in shorthand $\partial/\partial y(2.16)$ and then $\partial/\partial x(2.17)$) then substitute into (2.22)

$$
\begin{aligned}
\frac{\partial}{\partial y}(1.16): &\quad (\lambda+2\mu)\frac{\partial^2\Delta}{\partial x\partial y} + \mu\frac{\partial^2 W}{\partial y^2} + \rho\omega^2\frac{\partial u_x}{\partial y} = 0,\\
\implies &\quad \frac{\partial u_x}{\partial y} = \frac{1}{\rho\omega^2}\left[-\mu\frac{\partial^2 W}{\partial y^2} - (\lambda+2\mu)\frac{\partial^2\Delta}{\partial x\partial y}\right], \qquad (2.28)\\
\frac{\partial}{\partial x}(1.17): &\quad (\lambda+2\mu)\frac{\partial^2\Delta}{\partial x\partial y} - \mu\frac{\partial^2 W}{\partial x^2} + \rho\omega^2\frac{\partial u_y}{\partial x} = 0,\\
\implies &\quad \frac{\partial u_x}{\partial x} = \frac{1}{\rho\omega^2}\left[\mu\frac{\partial^2 W}{\partial x^2} - (\lambda+2\mu)\frac{\partial^2\Delta}{\partial x\partial y}\right]. \qquad (2.29)
\end{aligned}
$$

Now substitute (2.28), (2.29) into (2.22) and rearrange

$$
\begin{aligned}
\sigma_{xy} =&\mu\left(\frac{\partial u_x}{\partial y} + \frac{\partial u_y}{\partial x}\right),\\
=&\frac{\mu}{\rho\omega^2}\left[-\mu\frac{\partial^2 W}{\partial y^2} - (\lambda+2\mu)\frac{\partial^2\Delta}{\partial x\partial y} + \mu\frac{\partial^2 W}{\partial x^2} - (\lambda+2\mu)\frac{\partial^2\Delta}{\partial x\partial y}\right],\\
=&\frac{\mu^2}{\rho\omega^2}\left(\frac{\partial^2 W}{\partial x^2} - \frac{\partial^2 W}{\partial y^2} - 2\frac{\lambda+2\mu}{\mu}\frac{\partial^2\Delta}{\partial x\partial y}\right),\\
=&\frac{\mu^2}{\rho\omega^2}\left(\frac{\partial^2 W}{\partial x^2} - \frac{\partial^2 W}{\partial y^2} - 2k^2\frac{\partial^2\Delta}{\partial x\partial y}\right). \qquad (2.30)
\end{aligned}
$$

Where again $k^2 = (\lambda+2\mu)/\mu = k_2^2/k_1^2$.

The boundary conditions for the problem result from force being applied normal to the surface and being of unit magnitude in the region $|x|< a$. They are (omitting time variation),

$$
\sigma_{yy}(x,0) = \begin{cases} 1, & |x|< a \\ 0, & |x|> a \end{cases}, \quad \sigma_{xy}(x,0) = 0. \qquad (2.31)
$$

We note that, if for example the loading along the line were to be tangential, then the boundary conditions for $\sigma_{yy}(x,0)$ and $\sigma_{xy}(x,0)$ would in fact be swapped.

3 Fourier Transform to Exact Solution.

We will use the standard Fourier transform on the spacial variable x.

$$
\bar{f}(\xi) = \int_{-\infty}^{\infty} f(x)e^{-i\xi x}dx, \quad f(\xi) = \frac{1}{2\pi}\int_{-\infty}^{\infty}\bar{f}(x)e^{i\xi x}d\xi. \qquad (3.1)
$$

We note that

$$
F(f'(x,y)) = \int_{-\infty}^{\infty} f'(x,y)e^{-i\xi x}dx = \cancelto{0}{\left[f(x,y)e^{-i\xi x}\right]_{-\infty}^{\infty}} + i\xi\int_{-\infty}^{\infty} f(x,y)e^{-i\xi x}dx = i\xi\bar{f}(\xi,y)
$$

First with (2.16) we rearrange to obtain u_x then apply the transform,

$$
\begin{aligned}
(\lambda+2\mu)\frac{\partial \Delta}{\partial x}+\mu\frac{\partial W}{\partial y}+\rho\omega^2 u_x=0,&\\
\implies u_x=-\frac{1}{\rho\omega^2}\left[\mu\frac{\partial W}{\partial y}+(\lambda+2\mu)\frac{\partial \Delta}{\partial x}\right],&\\
=-\frac{\mu}{\rho\omega^2}\left[\frac{\partial W}{\partial y}+\frac{\lambda+2\mu}{\mu}\frac{\partial \Delta}{\partial x}\right],&\\
=-\frac{1}{k_2^2}\left[\frac{\partial W}{\partial y}+k^2\frac{\partial \Delta}{\partial x}\right],&\\
\implies \bar{u}_x=-\frac{1}{k_2^2}\left[\frac{d\bar{W}}{dy}+i\xi k^2\bar{\Delta}\right].& \qquad (3.2)
\end{aligned}
$$

Repeating for (1.17)

$$
\begin{aligned}
(\lambda+2\mu)\frac{\partial \Delta}{\partial y}-\mu\frac{\partial W}{\partial x}+\rho\omega^2 u_y=0,&\\
\implies u_y=-\frac{1}{\rho\omega^2}\left[(\lambda+2\mu)\frac{\partial \Delta}{\partial y}-\mu\frac{\partial W}{\partial x}\right],&\\
=-\frac{\mu}{\rho\omega^2}\left[\frac{\lambda+2\mu}{\mu}\frac{\partial \Delta}{\partial y}-\frac{\partial W}{\partial x}\right],&\\
=-\frac{1}{k_2^2}\left[k^2\frac{\partial \Delta}{\partial y}-\frac{\partial W}{\partial x}\right],&\\
\implies \bar{u}_y=-\frac{1}{k_2^2}\left[k^2\frac{d\bar{\Delta}}{dy}-i\xi\bar{W}\right].& \qquad (3.3)
\end{aligned}
$$

Now to transform the wave equations (2.18) and (2.19). Starting with (2.18) and noting that by a similar calculation as above $F(f''(x,y))=-\xi^2\bar{f}(\xi,y)$, hence

$$
\begin{aligned}
\nabla^2\Delta+k_1^2\Delta=0,&\\
\frac{\partial^2\Delta}{\partial x^2}+\frac{\partial^2\Delta}{\partial y^2}+k_1^2\Delta=0,&\\
\frac{d^2\bar{\Delta}}{dy^2}-\xi^2\bar{\Delta}+k_1^2\bar{\Delta}=0,&\\
\frac{d^2\bar{\Delta}}{dy^2}-(\xi^2+k_1^2)\bar{\Delta}=0.& \qquad (3.4)
\end{aligned}
$$

Now for (1.19)

$$
\begin{aligned}
\nabla^2 W+k_2^2 W=0,&\\
\frac{\partial^2 W}{\partial x^2}+\frac{\partial^2 W}{\partial y^2}+k_2^2 W=0,&\\
\frac{d^2\bar{W}}{dy^2}-\xi^2\bar{W}+k_2^2\bar{W}=0,&\\
\frac{d^2\bar{W}}{dy^2}-(\xi^2+k_2^2)\bar{W}=0.& \qquad (3.5)
\end{aligned}
$$

Now to transform the stresses (2.27) and (2.30) directly. First (2.27)

$$\sigma_{yy} = \frac{\mu^2}{\rho\omega^2}\left[2\frac{\partial^2 W}{\partial x \partial y} - k^4 \frac{\partial^2 \Delta}{\partial y^2} - k^2\left(k^2-2\right)\frac{\partial^2 \Delta}{\partial x^2}\right],$$

$$\bar{\sigma}_{yy} = \frac{\mu^2}{\rho\omega^2}\left[2i\xi\frac{d\bar{W}}{dy} - k^4 \frac{d\bar{\Delta}}{dy^2} + k^2\left(k^2-2\right)\xi^2\bar{\Delta}\right]. \tag{3.6}$$

Now (2.30)

$$\sigma_{xy} = \frac{\mu^2}{\rho\omega^2}\left(\frac{\partial^2 W}{\partial x^2} - \frac{\partial^2 W}{\partial y^2} - 2k^2\frac{\partial^2 \Delta}{\partial x \partial y}\right),$$

$$\bar{\sigma}_{xy} = -\frac{\mu^2}{\rho\omega^2}\left(\xi^2\bar{W} + \frac{d^2\bar{W}}{dy^2} + 2i\xi k^2\frac{d\bar{\Delta}}{dy}\right). \tag{3.7}$$

Using (2.31) we see the transformed boundary conditions are

$$\bar{\sigma}_{yy}(\xi,0) = \int_{-a}^{a} e^{-i\xi x}dx = -\left[\frac{e^{-i\xi x}}{i\xi}\right]_{-a}^{a} = \frac{1}{i\xi}\left(e^{i\xi a} - e^{-i\xi a}\right) = \frac{i}{\xi}\left(\cancel{\cos\xi a} + \sin\xi a - \cancel{\cos\xi a} + \sin\xi a\right),$$

$$\Longrightarrow\ \bar{\sigma}_{yy}(\xi,0) = \frac{2\sin\xi a}{\xi}, \quad \bar{\sigma}_{xy}(\xi,0) = 0. \tag{3.8}$$

Now to solve the transformed wave equations (3.4) and (3.5) where the positive exponential has been regarded as nonphysical as we require the decay condition of the wave and we wish not to have waves coming from infinity, so set $\tilde{A} = \tilde{B} = 0$.

$$\bar{\Delta} = Ae^{-(\xi^2-k_1^2)^{\frac{1}{2}}y} + \tilde{A}e^{(\xi^2-k_1^2)^{\frac{1}{2}}y} = Ae^{-(\xi^2-k_1^2)^{\frac{1}{2}}y}, \tag{3.9}$$

$$\bar{W} = Be^{-(\xi^2-k_2^2)^{\frac{1}{2}}y} + \tilde{B}e^{(\xi^2-k_2^2)^{\frac{1}{2}}y} = Be^{-(\xi^2-k_2^2)^{\frac{1}{2}}y}. \tag{3.10}$$

Now substitute (3.9) and (3.10), and their derivative's into the transformed stresses (3.6) and (3.7). Then evaluate at the transformed boundary conditions (3.8). To start we note that

$$\begin{aligned}
d\bar{\Delta}/dy &= -A(\xi^2-k_1^2)^{1/2}e^{-(\xi^2-k_1^2)^{1/2}y},\\
d\bar{W}/dy &= -B(\xi^2-k_2^2)^{1/2}e^{-(\xi^2-k_2^2)^{1/2}y},\\
d^2\bar{\Delta}/dy^2 &= A(\xi^2-k_1^2)e^{-(\xi^2-k_1^2)^{1/2}y},\\
d^2\bar{W}/dy^2 &= B(\xi^2-k_2^2)e^{-(\xi^2-k_2^2)^{1/2}y}.
\end{aligned}$$

Hence

$$\bar{\sigma}_{yy}(\xi,y) = \frac{\mu^2}{\rho\omega^2}\left[-2i\xi B(\xi^2-k_2^2)^{1/2}e^{-(\xi^2-k_2^2)^{1/2}y} - k^4A(\xi^2-k_1^2)e^{-(\xi^2-k_1^2)^{1/2}y} + k^2(k^2-2)\xi^2Ae^{-(\xi^2-k_1^2)^{1/2}y}\right],$$

$$\begin{aligned}
\bar{\sigma}_{yy}(\xi,0) &= \frac{\mu^2}{\rho\omega^2}\left[-2i\xi B(\xi^2-k_2^2)^{1/2} - k^4A(\xi^2-k_1^2) + k^2(k^2-2)\xi^2A\right],\\
&= \frac{2\sin\xi a}{\xi}.
\end{aligned} \tag{3.11}$$

$$\bar{\sigma}_{xy}(\xi,y) = -\frac{\mu^2}{\rho\omega^2}\left[\xi^2Be^{-(\xi^2-k_2^2)^{1/2}y} + B(\xi^2-k_2^2)e^{-(\xi^2-k_2^2)^{1/2}y} - 2i\xi k^2A(\xi^2-k_1^2)^{1/2}e^{-(\xi^2-k_1^2)^{1/2}y}\right],$$

$$\begin{aligned}
\bar{\sigma}_{xy}(\xi,0) &= \cancel{\frac{\mu^2}{\rho\omega^2}}\left[\xi^2B + B(\xi^2-k_2^2) - 2i\xi k^2A(\xi^2-k_1^2)^{1/2}\right],\\
&= 0.
\end{aligned} \tag{3.12}$$

Now solve (3.11) and (3.12) for A, B. From (3.11) we have

$$\frac{\mu^2}{\rho\omega^2}\left[A\left(k^2(k^2-2)\xi^2 - k^4(\xi^2-k_1^2)\right) - 2i\xi B(\xi^2-k_2^2)^{1/2}\right] = \frac{2\sin\xi a}{\xi},$$

$$A\left(k^2(k^2-2)\xi^2 - k^4(\xi^2-k_1^2)\right) = \frac{2\rho\omega^2\sin\xi a}{\xi\mu^2} + 2i\xi B(\xi^2-k_2^2)^{1/2},$$

$$A\xi\mu^2\left(k^2(k^2-2)\xi^2 - k^4(\xi^2-k_1^2)\right) = 2\rho\omega^2\sin\xi a + 2i\xi^2\mu^2 B(\xi^2-k_2^2)^{1/2},$$

$$A = \frac{2\rho\omega^2\sin\xi a + 2i\xi^2\mu^2 B(\xi^2-k_2^2)^{1/2}}{\xi\mu^2\left(k^2(k^2-2)\xi^2 - k^4(\xi^2-k_1^2)\right)},$$

$$A = \frac{2\rho\omega^2\sin\xi a}{\xi\mu^2\left(k^2(k^2-2)\xi^2 - k^4(\xi^2-k_1^2)\right)} + \frac{2i\xi^2\mu^2(\xi^2-k_2^2)^{1/2}}{\xi\mu^2\left(k^2(k^2-2)\xi^2 - k^4(\xi^2-k_1^2)\right)}B. \tag{3.13}$$

Similarly from (3.12)

$$B\left[\xi^2 + (\xi^2-k_2^2)\right] - 2i\xi k^2 A(\xi^2-k_1^2)^{1/2} = 0,$$

$$B = \frac{2i\xi k^2(\xi^2-k_1^2)^{1/2}}{(2\xi^2-k_2^2)}A. \tag{3.14}$$

Now to extract A, substitute (3.14) into (3.13)

$$A = \frac{2\rho\omega^2\sin\xi a}{\xi\mu^2\left(k^2(k^2-2)\xi^2 - k^4(\xi^2-k_1^2)\right)} + \frac{2i\xi^2\mu^2(\xi^2-k_2^2)^{1/2}}{\xi\mu^2\left(k^2(k^2-2)\xi^2 - k^4(\xi^2-k_1^2)\right)}\frac{2i\xi k^2(\xi^2-k_1^2)^{1/2}}{(2\xi^2-k_2^2)}A,$$

$$A = \frac{2\rho\omega^2\sin\xi a}{\xi\mu^2\left(k^2(k^2-2)\xi^2 - k^4(\xi^2-k_1^2)\right)} - \frac{4\xi^3\mu^2k^2(\xi^2-k_1^2)^{1/2}(\xi^2-k_2^2)^{1/2}}{\xi\mu^2\left(k^2(k^2-2)\xi^2 - k^4(\xi^2-k_1^2)\right)(2\xi^2-k_2^2)}A,$$

$$\frac{2\rho\omega^2\sin\xi a}{\xi\mu^2\left(k^2(k^2-2)\xi^2 - k^4(\xi^2-k_1^2)\right)} = A\left[1 + \frac{4\xi^3\mu^2k^2(\xi^2-k_1^2)^{1/2}(\xi^2-k_2^2)^{1/2}}{\xi\mu^2\left(k^2(k^2-2)\xi^2 - k^4(\xi^2-k_1^2)\right)(2\xi^2-k_2^2)}\right],$$

$$\begin{aligned}
&= A\left[\frac{\xi\mu^2\left(k^2(k^2-2)\xi^2 - k^4(\xi^2-k_1^2)\right)(2\xi^2-k_2^2) + 4\xi^3\mu^2k^2(\xi^2-k_1^2)^{1/2}(\xi^2-k_2^2)^{1/2}}{\xi\mu^2\left(k^2(k^2-2)\xi^2 - k^4(\xi^2-k_1^2)\right)(2\xi^2-k_2^2)}\right],\\
2\rho\omega^2\sin\xi a &= A\left[\frac{\xi\mu^2\left(k^2(k^2-2)\xi^2 - k^4(\xi^2-k_1^2)\right)(2\xi^2-k_2^2) + 4\xi^3\mu^2k^2(\xi^2-k_1^2)^{1/2}(\xi^2-k_2^2)^{1/2}}{(2\xi^2-k_2^2)}\right],\\
&= A\left[\frac{-\xi\mu^2\left(k^2(k^2-2)\xi^2 - k^4(\xi^2-k_1^2)\right)(2\xi^2-k_2^2) - 4\xi^3\mu^2k^2(\xi^2-k_1^2)^{1/2}(\xi^2-k_2^2)^{1/2}}{(k_2^2-2\xi^2)}\right],\\
2\rho\omega^2(k_2^2-2\xi^2)\sin\xi a &= A\left[-\xi\mu^2\left(k^2(k^2-2)\xi^2 - k^4(\xi^2-k_1^2)\right)(2\xi^2-k_2^2) - 4\xi^3\mu^2k^2(\xi^2-k_1^2)^{1/2}(\xi^2-k_2^2)^{1/2}\right],\\
&= A\left[\xi\mu^2\left(-k^2(k^2-2)\xi^2 + k^2(k^2\xi^2-k^2k_1^2)\right)(2\xi^2-k_2^2) - 4\xi^3\mu^2k^2(\xi^2-k_1^2)^{1/2}(\xi^2-k_2^2)^{1/2}\right],\\
&= A\left[\xi\mu^2k^2\left(-k^2\xi^2 + 2\xi^2 + k^2\xi^2 - k^2k_1^2\right)(2\xi^2-k_2^2) - 4\xi^3\mu^2k^2(\xi^2-k_1^2)^{1/2}(\xi^2-k_2^2)^{1/2}\right],\\
&= A\left[\xi\mu^2k^2\left(2\xi^2 - k^2k_1^2\right)(2\xi^2-k_2^2) - 4\xi^3\mu^2k^2(\xi^2-k_1^2)^{1/2}(\xi^2-k_2^2)^{1/2}\right],\\
&= A\left[\xi\mu^2k^2\left(2\xi^2 - k_2^2\right)(2\xi^2-k_2^2) - 4\xi^3\mu^2k^2(\xi^2-k_1^2)^{1/2}(\xi^2-k_2^2)^{1/2}\right],\\
&= A\xi\mu^2k^2\left[\left(2\xi^2-k_2^2\right)^2 - 4\xi^2(\xi^2-k_1^2)^{1/2}(\xi^2-k_2^2)^{1/2}\right],\\
&= A\xi\mu^2k^2F(\xi),
\end{aligned}$$

$$\implies A = \frac{2\rho\omega^2(k_2^2 - 2\xi^2)}{\mu^2 k^2 \xi F(\xi)} \sin \xi a.$$

With $F(\xi) = \left(2\xi^2 - k_2^2\right)^2 - 4\xi^2(\xi^2 - k_1^2)^{1/2}(\xi^2 - k_2^2)^{1/2}$, hence with transformed dilatation $\bar{\Delta}$ is

$$\bar{\Delta} = \frac{2\rho\omega^2(k_2^2 - 2\xi^2)}{\mu^2 k^2 \xi F(\xi)} \sin(\xi a) e^{-(\xi^2 - k_1^2)^{1/2} y}. \tag{3.15}$$

Similarly extract B by substitution of (3.13) into (3.14)

$$\begin{aligned}
B &= \frac{2i\xi k^2(\xi^2 - k_1^2)^{1/2}}{(2\xi^2 - k_2^2)} \left(\frac{2\rho\omega^2 \sin \xi a}{\xi\mu^2 \left(k^2(k^2-2)\xi^2 - k^4(\xi^2 - k_1^2)\right)} + \frac{2i\xi^2\mu^2(\xi^2 - k_2^2)^{1/2}}{\xi\mu^2 \left(k^2(k^2-2)\xi^2 - k^4(\xi^2 - k_1^2)\right)} B \right), \\
B &= \frac{4i\xi k^2(\xi^2 - k_1^2)^{1/2}\rho\omega^2 \sin \xi a}{(2\xi^2 - k_2^2)\xi\mu^2 \left(k^2(k^2-2)\xi^2 - k^4(\xi^2 - k_1^2)\right)} - \frac{4\xi^3\mu^2 k^2(\xi^2 - k_1^2)^{1/2}(\xi^2 - k_2^2)^{1/2}}{(2\xi^2 - k_2^2)\xi\mu^2 \left(k^2(k^2-2)\xi^2 - k^4(\xi^2 - k_1^2)\right)} B, \\
B &\left[1 + \frac{4\xi^3\mu^2 k^2(\xi^2 - k_1^2)^{1/2}(\xi^2 - k_2^2)^{1/2}}{(2\xi^2 - k_2^2)\xi\mu^2 \left(k^2(k^2-2)\xi^2 - k^4(\xi^2 - k_1^2)\right)}\right] = \frac{4i\xi k^2(\xi^2 - k_1^2)^{1/2}\rho\omega^2 \sin \xi a}{(2\xi^2 - k_2^2)\xi\mu^2 \left(k^2(k^2-2)\xi^2 - k^4(\xi^2 - k_1^2)\right)},
\end{aligned}$$

$$\begin{aligned}
B \left[(2\xi^2 - k_2^2)\xi\mu^2 \left(k^2(k^2-2)\xi^2 - k^4(\xi^2 - k_1^2)\right) + 4\xi^3\mu^2 k^2(\xi^2 - k_1^2)^{1/2}(\xi^2 - k_2^2)^{1/2}\right] =& 4i\xi k^2(\xi^2 - k_1^2)^{1/2}\rho\omega^2 \sin \xi a, \\
B \left[(2\xi^2 - k_2^2)\mu^2 \left((k^2-2)\xi^2 - k^2(\xi^2 - k_1^2)\right) + 4\xi^2\mu^2(\xi^2 - k_1^2)^{1/2}(\xi^2 - k_2^2)^{1/2}\right] =& 4i(\xi^2 - k_1^2)^{1/2}\rho\omega^2 \sin \xi a, \\
B \left[(2\xi^2 - k_2^2)\mu^2 \left(-k^2\xi^2 + 2\xi^2 + k^2\xi^2 - k_1^2\right) - 4\xi^2\mu^2(\xi^2 - k_1^2)^{1/2}(\xi^2 - k_2^2)^{1/2}\right] =& -4i(\xi^2 - k_1^2)^{1/2}\rho\omega^2 \sin \xi a, \\
B\mu^2 \left[\left(2\xi^2 - k_1^2\right)^2 - 4\xi^2(\xi^2 - k_1^2)^{1/2}(\xi^2 - k_2^2)^{1/2}\right] =& \\
B\mu^2 F(\xi) =&
\end{aligned}$$

$$\implies B = -\frac{4i(\xi^2 - k_1^2)^{1/2}\rho\omega^2}{\mu^2 F(\xi)} \sin \xi a.$$

Hence,

$$\bar{W} = -\frac{4i(\xi^2 - k_1^2)^{1/2}\rho\omega^2}{\mu^2 F(\xi)} \sin(\xi a) e^{-(\xi^2 - k_2^2)^{1/2} y}.$$

We note that

$$d\bar{W}/dy = \frac{4i(\xi^2 - k_1^2)^{1/2}(\xi^2 - k_2^2)^{1/2}\rho\omega^2}{\mu^2 F(\xi)} \sin(\xi a) e^{-(\xi^2 - k_2^2)^{1/2} y},$$

and

$$d\bar{\Delta}/dy = -\frac{2\rho\omega^2(k_2^2 - 2\xi^2)(\xi^2 - k_1^2)^{1/2}}{\mu^2 k^2 \xi F(\xi)} \sin(\xi a) e^{-(\xi^2 - k_1^2)^{1/2} y}.$$

Thus the transformed displacement $\bar{u}_x$ (3.2) is given by

$$\begin{aligned}
\bar{u}_x = -\frac{1}{k_2^2} \Bigg[&\frac{4i(\xi^2 - k_1^2)^{1/2}(\xi^2 - k_2^2)^{1/2}\rho\omega^2}{\mu^2 F(\xi)} \sin(\xi a) e^{-(\xi^2 - k_2^2)^{1/2} y} \\
&+ i\xi k^2 \left(\frac{2\rho\omega^2(k_2^2 - 2\xi^2)}{\mu^2 k^2 \xi F(\xi)} \sin(\xi a) e^{-(\xi^2 - k_1^2)^{1/2} y} \right) \Bigg],
\end{aligned}$$

$$\begin{aligned}
\bar{u}_x &= -\frac{2 \sin \xi a}{\mu F(\xi)} \left[2i(\xi^2 - k_1^2)^{1/2}(\xi^2 - k_2^2)^{1/2} e^{-(\xi^2 - k_2^2)^{1/2} y} + i(k_2^2 - 2\xi^2) e^{-(\xi^2 - k_1^2)^{1/2} y} \right], \\
\bar{u}_x &= \frac{2 \sin \xi a}{i\mu F(\xi)} \left[2(\xi^2 - k_1^2)^{1/2}(\xi^2 - k_2^2)^{1/2} e^{-(\xi^2 - k_2^2)^{1/2} y} + (k_2^2 - 2\xi^2) e^{-(\xi^2 - k_1^2)^{1/2} y} \right].
\end{aligned} \tag{3.16}$$

Similarly for $\bar{u}_y$ (3.3)

$$\bar{u}_y = -\frac{1}{k_2^2}\left[k^2\left(-\frac{2\rho\omega^2(k_2^2-2\xi^2)(\xi^2-k_1^2)^{1/2}}{\mu^2 k^2\xi F(\xi)}\sin(\xi a)e^{-(\xi^2-k_1^2)^{1/2}y}\right)\right.$$
$$\left. - i\xi\left(-\frac{4i(\xi^2-k_1^2)^{1/2}\rho\omega^2}{\mu^2 F(\xi)}\sin(\xi a)e^{-(\xi^2-k_2^2)^{1/2}y}\right)\right]$$

$$\bar{u}_y = -\frac{2(\xi^2-k_1^2)^{1/2}\sin(\xi a)}{\mu^2 k_2^2 F(\xi)}\left[-\frac{\rho\omega^2(k_2^2-2\xi^2)}{\xi}e^{-(\xi^2-k_1^2)^{1/2}y} - 2\xi\rho\omega^2 e^{-(\xi^2-k_2^2)^{1/2}y}\right]$$

$$\bar{u}_y = \frac{2(\xi^2-k_1^2)^{1/2}\sin(\xi a)}{\mu F(\xi)}\left[\frac{(k_2^2-2\xi^2)}{\xi}e^{-(\xi^2-k_1^2)^{1/2}y} + 2\xi e^{-(\xi^2-k_2^2)^{1/2}y}\right]$$

$$\bar{u}_y = \frac{2(\xi^2-k_1^2)^{1/2}\sin(\xi a)}{\mu\xi F(\xi)}\left[(k_2^2-2\xi^2)e^{-(\xi^2-k_1^2)^{1/2}y} + 2\xi^2 e^{-(\xi^2-k_2^2)^{1/2}y}\right] \tag{3.17}$$

Now we obtain u_x, u_y by using the inverse Fourier transform (3.1) on (3.16) and (3.17). The exact displacements are

$$u_x(x,y) = \frac{1}{i\mu\pi}\int_{-\infty}^{\infty}\frac{\sin\xi a}{F_0(\xi)}\left[2(\xi^2-1)^{1/2}(\xi^2-k^2)^{1/2}e^{-(\xi^2-k^2)^{1/2}y} + (k^2-2\xi^2)e^{-(\xi^2-1)^{1/2}y}\right]e^{i\xi x}d\xi, \tag{3.18}$$

$$u_y(x,y) = \frac{1}{\mu\pi}\int_{-\infty}^{\infty}\frac{(\xi^2-1)^{1/2}\sin\xi a}{\xi F_0(\xi)}\left[(k^2-2\xi^2)e^{-(\xi^2-1)^{1/2}y} + 2\xi^2 e^{-(\xi^2-k^2)^{1/2}y}\right]e^{i\xi x}d\xi. \tag{3.19}$$

Where $F_0(\xi) = \left(2\xi^2-k^2\right)^2 - 4\xi^2(\xi^2-1)^{1/2}(\xi^2-k^2)^{1/2}$.

Note that we have chosen k_1 as a normalising factor for all length parameters. i.e., $k_1^2=1$, $k^2=k_2^2$. This can be done because k_1, k_2 have units of reciprocal length. And it should also be understood that $x \sim k_1 x$, $y \sim k_1 y$, $\xi \sim \xi/k_1$ in the preceding. This is due to the fact these integrals change most rapidly around $k_1 = 1$ as we will see.

Later, to recover the results for the displacements, we will let $a \to 0$ but letting the load per unit length $2a$ be constant, i.e., pressure remains constant. thus in (3.18) and (3.19) $\sin\xi a$ is replaced by ξa and $\sin\xi a/\xi$ is replaced by a, from Taylor expansion.

4 Poles, Branch Points, and the Branch Cut.

The poles of (3.18) and (3.19) are determined by $F_0(\xi) = 0$, which are given by $\xi = \pm\xi_R \in \mathbb{R}$. To find the poles we must choose a suitable value of k. This is given by the material parameters of our solid. For convenience we express k in terms of Poisson's ratio. To this end we have

$$\lambda = \frac{E\nu}{(1+\nu)(1-2\nu)}, \quad \mu = \frac{E}{2(1+\nu)}$$

where E is Young's modulus and ν is Poisson's ratio. Substituting these into $k^2 = (\lambda+2\mu)/\mu$ yields

$$k^2 = \frac{2\nu(1+\nu)}{(1+\nu)(1-\nu)} + \frac{2(1+\nu)}{(1+\nu)} = \frac{2(1-\nu)}{1-2\nu}$$

Common values for solids are $\nu = 1/4$, or $\nu = 1/3$ (i.e., $k=\sqrt{3}$, $k^2=4$ respectively). These are used to numerically obtain values for ξ_R. We will approximate these roots with Newton–Raphson iteration

$$a_{n+1} = a_n - F_0(a_n)/F_0'(a_n).$$

And will only consider the case for $k=\sqrt{3}$ for illustration. Various other techniques and use of modern software are, of-course perfectly viable, with the latter being useful when high precision is needed. First we need to find $F_0'(\xi)$

$$F_0'(\xi)=8\xi(2\xi^2-3)-8\xi(\xi^2-1)^{1/2}(\xi^2-3)^{1/2}-\frac{4\xi^3(\xi^2-3)^{1/2}}{(\xi^2-1)^{1/2}}-\frac{4\xi^3(\xi^2-1)^{1/2}}{(\xi^2-3)^{1/2}}.$$

Let $\xi_R=\xi_0=2$, we have

$$\xi_1=2-\frac{F_0(2)}{F_0'(2)}=1.874486111,$$

and so on using this iterative relation until we obtain $\xi_R\sim 1.8839$. And then repeat starting with -2 to get the negative term. We obtain $\xi_R=\pm 1.8839$, and $\xi_R=\pm 2.1447$ for $\nu=1/4$, or $\nu=1/3$ (i.e., $k=\sqrt{3}$, $k=2$ respectively. It should also be noted that in general $\nu>0.263...$ will lead to 1 real root and 2 complex roots, and $\nu<0.263...$ will lead to 3 real roots (due to squaring of $F_0(\xi)$). However any resulting complex roots are disregarded here as they lead to damping with respect to time; which is not the case in the present problem.

The location of the branch points will be determined by $(\xi^2-1)^{1/2}$ and $(\xi^2-k^2)^{1/2}$, i.e., $\xi=\pm 1,\ \pm k$. We introduce the functions $\alpha(\xi)=(\xi^2-1)^{1/2}$ and $\beta(\xi)=(\xi^2-k^2)^{1/2}$. Hence we have $e^{-\alpha y}$, $e^{-\beta y}$ in (2.19), (2.20). As we require the decay condition, we need the real parts of α, β to always be greater than zero. Initially, with small damping being included in the system, the branch cuts will lie along hyperbolas. These hyperbolas will degenerate to cuts along the real and imaginary axis as the damping tends to zero. I will illustrate this via a generalisation which extends to the current problem. If we have branch points located at some $\xi=\pm b$ given by some $\gamma=(\xi^2-b)^{1/2}$, located on the real axis, we can let $b^2=\tilde{b}^2$, where $\tilde{b}^2$ is complex and given by

$$\tilde{b}=a-ih,\quad (a,h>0). \tag{4.1}$$

Now with $\tilde{b}^2$ complex the branch points $\xi=\pm b$ are moved off the real axis and into the second and fourth quadrants. In this generalised case we have in our integrals $e^{-\gamma y}$, with $y>0$. if we let

$$\gamma=X+iY,\quad \gamma^2=X^2-Y^2+2iXY,$$

we will have the cuts given by Re $\gamma=0$, which implies

$$\mathrm{Re}\gamma^2\le 0,\quad \mathrm{Im}\gamma^2=0. \tag{4.2}$$

Letting $\xi=\zeta+i\eta$ and using (4.1) we can write

$$\gamma^2=\zeta^2-\eta^2+2i\zeta\eta-a^2+h^2+2iah.$$

Thus, from (4.2) we have

$$\mathrm{Re}\gamma^2=\zeta^2-\eta^2-a^2+h^2\le 0,\quad \mathrm{Im}\gamma^2=\zeta\eta+ah=0.$$

From the second equation we see the branch cuts are given by hyperbolas (one for $a,h>0$, and the other for $a,h<0$), which pass through the branch points. The second equation shows us which portion the hyperbolas must be cut along. Finally we let $\tilde{b}$ be real, i.e., $h\to 0$. We get

$$\zeta^2-\eta^2-a^2\le 0,\quad \zeta\eta=0.$$

If $\xi=0$, then $\eta^2\le a^2$, and if $\eta=0$, then $-\xi^2\le a^2$. And thus our hyperbolic cuts have cuts along the real and imaginary axis as the damping tended to zero.

Now moving back to our problem we do this same procedure branch points located at $\xi=\pm 1,\ \pm k$ and to obtain our cuts. Then the entire contour integral is given by

$$\oint=\int_{\Gamma_1}+\int_{\Gamma_\alpha}+\int_{\Gamma_\beta}+\int_{\Gamma_2}+\int_{-R}^{R}=-2\pi i\sum\mathrm{Res}, \tag{4.3}$$

We assume $x > 0$ so that the contour is closed in the upper half plane. Poles at $\xi = \pm\xi_R$ are, respectively, excluded and included from our contour. This is because by convention we have the pole at $-\xi_R$ representing waves coming from the origin and the pole at $-\xi_R$ representing waves coming in from infinity. Geometry around the branch points remains to be determined using the method of steepest descent.

Contribution from the poles will (where we will use Cauchy's residue theorem) lead to surface waves, and contribution from the branch cuts lead to interior waves in the far field, where we will neglect the contribution from the poles using the method of steepest descent. This is because we see in the residues of the poles a factor of $e^{-Rg\cos\theta}$ where $g = g(\xi_R, m)$ and $m = 1$ or k. Thus in the limit problem of $R \to \infty$ this term is negligible, apart from the case when $\theta = \pi/2$ where it is in fact the dominant term. Hence, in the limit problem (the far field), contribution from the branch cut integrals specifically corresponds to the interior waves and not the surface waves. When we consider surface waves alone, as contribution from the poles is the dominant term, we can neglect contribution from the branch cut integrals. Hence we consider the cases separately. Contribution from Γ_1, Γ_2 will vanish. Contribution along the real axis is what we are interested in, as the major contribution comes from a small region $f'(\xi) = 0$ (see (5.2)) for large x, away from this point rapid increasing oscillations of the integrand are assumed to cancel by interference. From here then the main task is evaluation of the branch cut integrals. Then we will consider the case of surface waves, where we shall see resolving these is much simpler. See Graff [1991] [pp. 348] for more details on the geometry of the contour and the branch cut.

5 Evaluation of Branch Cut Integrals.

In general most wave propagation problems are too complex for exact solutions to be found; The same is true for this problem. Approximate solutions to (3.18) and (3.19) will be found using the method of steepest descent. This method will be used to find the far field displacement. We see (3.18) and (3.19) have the form

$$I_1 = \int_{-\infty}^{\infty} \chi(\xi) e^{i\xi x - (\xi^2 - m)^{1/2} y} d\xi. \tag{5.1}$$

where $m = 1$ or k. Introducing polar coordinates $x = R\sin\theta$, $y = R\cos\theta$ where θ is measured from the y-axis. Then

$$I_1 = \int_{-\infty}^{\infty} \chi(\xi) e^{i\xi R\sin\theta - (\xi^2 - m)^{1/2} R\cos\theta} d\xi = \int_{-\infty}^{\infty} \chi(\xi) e^{Rf(\xi)} d\xi. \tag{5.2}$$

Where $f(\xi) = i\xi\sin\theta - (\xi^2 - m)^{1/2}\cos\theta$.

We need to deform the original contour into a new one along the steepest descent path through the saddle points so that a large contribution of the integral comes from a short portion of the path in the vicinity of that point. This new deformed path will have the key property of constant f_2, where f_2 is the imaginary part of $f(\xi)$. To achieve this we perform a change of variables such that our contour has been deformed through these saddle points of $f(\xi)$. In this transformed form our integral I_1 can be approximated using asymptotic methods, in this case, an alternate form of Watson's lemma will be used. Note that if f_2 were to be oscillatory and, for large R, these dense oscillations may negate the contributions of the real part. Determining the shape of the new deformed contour is also key so we can strategically include and exclude various points on our path.

Continuing on, we perform a change in variables and write $f(\xi) = f_1 + if_2 = -(\xi^2 - m)^{1/2}\cos\theta + i\xi\sin\theta \implies f_1 = -(\xi^2 - m)^{1/2}\cos\theta,\ f_2 = \xi\sin\theta$, we then have

$$I_1 = \int_{-\infty}^{\infty} \chi(\xi) e^{R(f_1 + if_2)} d\xi = \int_{-\infty}^{\infty} \chi(\xi) e^{Rf_1} e^{iRf_2} d\xi.$$

We wish to maximise the contribution from e^{Rf_1} at a point along the deformed contour. Away from this point we wish the contribution to decrease rapidly.

As we can see saddle points are the key aspect to this method. It is therefor key to understand their properties. Consider the real and imaginary parts of $f(\xi)$ given by

$$f_1 = f_1(\zeta, \eta), \quad f_2 = f_2(\zeta, \eta).$$

The gradient of f_1 is given by

$$\nabla f_1 = \frac{\partial f_1}{\partial \zeta}\mathbf{i} + \frac{\partial f_1}{\partial \eta}\mathbf{j}.$$

This represents the direction of maximum change in f_1. The unit vector in this direction is given by

$$\mathbf{n}_1 = \frac{\nabla f_1}{|\nabla f_1|}$$

Naturally the direction of $\mathbf{n}_1$ is always orthogonal to contour lines of f_1, these are called slowness contours. This direction is given as $\mathbf{s}_1$ where

$$\mathbf{n}_1 \cdot \mathbf{s}_1 = 0, \quad \mathbf{s}_1 = \frac{1}{|\nabla f_1|}\left(-\frac{\partial f_1}{\partial \eta}\mathbf{i} + \frac{\partial f_1}{\partial \zeta}\mathbf{j}\right),$$

where we have used $(x, y) \mapsto (-y, x)$. Now it maybe shown that $\mathbf{n}_1$ is a scalar multiple of, and hence parallel to, the direction of constant f_2. Thus

$$\nabla f_2 = \frac{\partial f_2}{\partial \zeta}\mathbf{i} + \frac{\partial f_2}{\partial \eta}\mathbf{j},$$

and

$$\mathbf{n}_2 = \frac{\nabla f_2}{|\nabla f_2|}, \quad \mathbf{s}_2 = \frac{1}{|\nabla f_2|}\left(-\frac{\partial f_2}{\partial \eta}\mathbf{i} + \frac{\partial f_2}{\partial \zeta}\mathbf{j}\right).$$

With $\mathbf{s}_2$ direction of constant f_2. However, from Cauchy-Riemann equations,

$$\frac{\partial f_1}{\partial \zeta} = \frac{\partial f_2}{\partial \eta}, \quad \frac{\partial f_1}{\partial \eta} = -\frac{\partial f_2}{\partial \zeta},$$

implies

$$\mathbf{s}_2 = -\frac{1}{|\nabla f_2|}\left(\frac{\partial f_1}{\partial \zeta}\mathbf{i} + \frac{\partial f_1}{\partial \eta}\mathbf{j}\right).$$

Thus, $\mathbf{s}_2$ parallel to $\mathbf{n}_1$. This is important in removing oscillations of e^{iRf_2} along the strategic path. We have the extreme values of f_1 occurring for $\nabla f_1 = 0$ or

$$\frac{\partial f_1}{\partial \zeta} = \frac{\partial f_2}{\partial \eta} = 0.$$

The Cauchy-Riemann equations are satisfied in any direction $\mathbf{n}$ and $\mathbf{s}$, so at an extreme we have

$$\frac{\partial f_1}{\partial n} = \frac{\partial f_1}{\partial s} = 0.$$

It also follows from Cauchy-Riemann equations that f_2 will be stationary and, generally, $df/d\xi = 0$. The only way f_1 can satisfy the above equation and not violate the maximum-modulus theorem of complex variables (f_1, f_2 cannot attain local max/min within a contour C, but can in fact attain extreme values on C) is to pass through a 'saddle point' (P_s). We see at P_s the gradient is locally zero. However, passing through P_s in one direction leads to local max, but in the other direction it leads to local min. (Imagine a Pringle, traversing across the short axis leads to local max, but traversing the long axis leads to local min, or vice versa depending which side faces up). The key aspect is that directions of constant f_2 coincide with max/min directions of f_1.

To understand this local topology of a saddle point further we can Taylor expand $f(\xi)$ about the saddle point ξ_0

$$f(\xi) = f(\xi_0) + f'(\xi_0)(\xi - \xi_0) + \frac{f''(\xi_0)(\xi - \xi_0)^2}{2} + \dots \; .$$

However as we are at a saddle point we have $f'(\xi_0) = 0$. We assume that $f''(\xi_0) \neq 0$, and (for now) let

$$\frac{f''(\xi_0)}{2} = a_2 e^{i\alpha_2}, \quad \xi - \xi_0 = re^{i\theta}.$$

Then by substituting these back we have for $f(\xi)$, $f_1(\xi)$ in neighborhood of ξ_0

$$f(\xi) = f(\xi_0) + a_2 r^2 e^{i(2\theta + \alpha_2)},$$

$$f_1(\xi_0) = \mathrm{Re}\, f(\xi_0) + a_2 r^2 \cos(2\theta + \alpha_2).$$

We see as θ goes from 0 to 2π about ξ_0, f_1 will attain two maxima and two minima. The contour lines of f_1 are given by $\cos(2\theta + \alpha_2) = 0$. We find there are two such lines at $45°$ with respect to the min/max directions. The maximum direction are contour of $f_1 > f_1(\xi_0)$, and minimum directions are for $f_1 < f_1(\xi_0)$, and locally, we these are families of hyperbolas. Finally we have

$$f_2 = \mathrm{Im}\, f(\xi_0) + a_2 r^2 e^{i(2\theta + \alpha_2)}.$$

Next, we deform our contour along the steepest descent path, such that it passes through the saddle point. We have

$$f(\xi) = f_1(\xi) + i f_2(\xi_0). \tag{5.3}$$

So f_2 is constant here. And,

$$f_1(\xi) = f_1(\xi_0) - p. \tag{5.4}$$

Where $0 < p < 1$ is some small perturbation around our saddle point. Now substituting (5.4) into (5.3)

$$f(\xi) = f_1(\xi_0) - p + i f_2(\xi_0). \tag{5.5}$$

Which is nothing more than

$$f(\xi) = f(\xi_0) - p, \tag{5.6}$$

where we have used $f(\xi_0) = f_1(\xi_0) + i f_2(\xi_0)$. Now we apply a change of variables, where for convenience we write $p = u^2$ ($p > 0$; $u^2 > 0$), so

$$f(\xi) = f(\xi_0) - u^2. \tag{5.7}$$

Next we can use this result and substitute into (5.2),

$$I_1 = \int_{-\infty}^{\infty} \chi(\xi(u)) e^{Rf(\xi_0)} e^{-Ru^2} \frac{d\xi}{du} du. \tag{5.8}$$

$e^{Rf(\xi_0)}$ is constant, hence

$$I_1 = e^{Rf(\xi_0)} \int_{-\infty}^{\infty} \chi(\xi(u)) e^{-Ru^2} \frac{d\xi}{du} du. \tag{5.9}$$

Note the aim here is to have the majority of the contribution come from the exponential term. Now it is desired to obtain a simpler expression for u. To this end consider the Taylor expansion for $f(\xi)$ at our saddle point.

$$f(\xi) = f(\xi_0) + f'(\xi_0)(\xi - \xi_0) + \frac{1}{2} f''(\xi_0)(\xi - \xi_0)^2 + \mathcal{O}((\xi - \xi_0)^3). \tag{5.10}$$

As we are at a saddle point we have $f' = 0$ and we assume $f'' \neq 0$. Hence

$$f(\xi) = f(\xi_0) + \frac{1}{2}f''(\xi_0)(\xi - \xi_0)^2, \tag{5.11}$$

$$f(\xi) - f(\xi_0) = -u^2 = \frac{1}{2}f''(\xi_0)(\xi - \xi_0)^2,$$

$$u^2 = -\frac{1}{2}f''(\xi_0)(\xi - \xi_0)^2. \tag{5.12}$$

Where we have used (5.7). Now we switch to polar coordinates, and let

$$(\xi - \xi_0) = re^{i\theta}, \tag{5.13}$$

$$(\xi - \xi_0)^2 = r^2e^{2i\theta}. \tag{5.14}$$

Thus (5.12) becomes,

$$u^2 = -\frac{1}{2}f''(\xi_0)r^2e^{2i\theta}. \tag{5.15}$$

Now shifting our attention to writing $f''(\xi_0)$ in polar, we see

$$f''(\xi_0) = |f''(\xi_0)|e^{i\beta}. \tag{5.16}$$

This comes from $z = |z|e^{i\arg(z)}$, Where z is some complex valued number. Substitute this result into (5.15),

$$u^2 = -\frac{1}{2}|f''(\xi_0)|r^2e^{i(\beta+2\theta)} = -\frac{1}{2}|f''(\xi_0)|r^2e^{i\varphi}. \tag{5.17}$$

Since $u > 0$, and therefor real, this implies $e^{-i\phi} = -1$ which implies $\phi = \pm\pi$, hence

$$u^2 = \frac{1}{2}|f''(\xi_0)|r^2, \tag{5.18}$$

$$u = \pm\frac{1}{\sqrt{2}}|f''(\xi_0)|^{1/2}r. \tag{5.19}$$

From (4.13) we see $r = (\xi - \xi_0)e^{-i\theta}$, thus

$$u = \pm\frac{|f''(\xi_0)|^{1/2}}{\sqrt{2}}(\xi - \xi_0)e^{-i\theta}. \tag{5.20}$$

Now we can finally take the derivative

$$\frac{du}{d\xi} = \pm\frac{|f''(\xi_0)|^{1/2}}{\sqrt{2}}e^{-i\theta}, \tag{5.21}$$

$$\implies \frac{d\xi}{du} = \pm\frac{\sqrt{2}e^{i\theta}}{|f''(\xi_0)|^{1/2}}. \tag{5.22}$$

Which yields for I_1 (using (5.9 and (5.22))

$$I_1 = \pm\, e^{Rf(\xi_0)}\int_{-\infty}^{\infty}\chi(\xi(u))e^{-Ru^2}\frac{\sqrt{2}e^{i\theta}}{|f''(\xi_0)|^{1/2}}du, \tag{5.23}$$

$$= \pm\,\frac{\sqrt{2}e^{i\theta}e^{Rf(\xi_0)}}{|f''(\xi_0)|^{1/2}}\int_{-\infty}^{\infty}\chi(\xi(u))e^{-Ru^2}du. \tag{5.24}$$

Selection of proper sign depends on which direction we pass through the saddle point (+45° for positive sign, −135° for negative sign with respect to the real ξ-axis). If after passing through the saddle point u is positive then the positive sign must be selected. For now we will leave it as $\pm$. Thus, This is finally a form which can be evaluated asymptotically using a version of Watson's lemma as found in Copson [1962] [pp. 14-18]. We have

$$J = \int_{-A}^{B} e^{-\frac{a^2}{2}z^2} f(z)dz, \tag{5.25}$$

with A, B positive. Put $z = \tau^{1/2}$ in $(0, B)$ and $z = -\tau^{1/2}$ in $(-A, 0)$; then

$$J = \frac{1}{2}\int_{0}^{A^2} e^{-\frac{a^2}{2}\tau} f(-\tau^{1/2})\tau^{-1/2}d\tau + \frac{1}{2}\int_{0}^{B^2} e^{-\frac{a^2}{2}\tau} f(\tau^{1/2})\tau^{-1/2}d\tau. \tag{5.26}$$

Which is then expanded normally where contributions from odd powers of $\tau^{1/2}$ in $f(\tau^{1/2})$ cancel; then

$$J \sim \frac{1}{2}\int_{0}^{Z} e^{-\frac{a^2}{2}\tau}\tau^{-1/2}(a_0 + a_2\tau + ... + a_{2n}\tau^n + ...)d\tau, \tag{5.27}$$

or

$$J \sim \sum_{n=0}^{\infty} a_{2n}\frac{(n+\frac{1}{2})!}{(\frac{1}{2}a^2)^{n+1/2}} = \frac{\sqrt{2\pi}}{a}\left(a_0 + \frac{a_2}{a^2} + \frac{3\sqrt{\pi}}{4}\frac{a_4}{a^4} + ...\right). \tag{5.28}$$

Comparing this to I_1 in (5.24) we have $a^2 = 2R$ and we are expanding $\chi(u)$. Noting this we directly find

$$I_1 \sim \pm\frac{\sqrt{2}e^{i\theta}e^{Rf(\xi_0)}}{|f''(\xi_0)|^{1/2}}\sum_{n=0}^{\infty}\chi^{(2n)}(u)\frac{(n-\frac{1}{2})!}{R^{n+1/2}}, \tag{5.29}$$

or

$$I_1 \sim \pm\frac{\sqrt{2}e^{i\theta}e^{Rf(\xi_0)}}{|f''(\xi_0)|^{1/2}}\left(\chi(0)\frac{\sqrt{\pi}}{R^{1/2}} + \chi''(0)\frac{\sqrt{\pi}}{2R^{3/2}} + \chi^{(4)}(0)\frac{3\sqrt{\pi}}{4R^{5/2}} + ...\right), \tag{5.30}$$

or

$$I_1 \sim e^{Rf(\xi_0)}\frac{d\xi}{du}\left(\chi(0)\frac{\sqrt{\pi}}{R^{1/2}} + \chi''(0)\frac{\sqrt{\pi}}{2R^{3/2}} + \chi^{(4)}(0)\frac{3\sqrt{\pi}}{4R^{5/2}} + ...\right). \tag{5.31}$$

We now determine the saddle points of $f(\xi)$ from $df(\xi)/d\xi = 0$

$$\frac{df(\xi)}{d\xi} = i\sin\theta - \frac{\xi\cos\theta}{(\xi^2-m)^{1/2}} = 0 \implies i\sin(\theta) = \frac{\xi\cos\theta}{(\xi^2-m)^{1/2}}$$

$$-\sin^2(\theta) = \frac{\xi^2\cos^2\theta}{(\xi^2-m)} \implies -(\xi^2-m^2)\sin^2\theta = \xi^2\cos^2\theta$$

$$-\xi^2\sin^2\theta + m^2\sin^2\theta = \xi^2\cos^2\theta \implies m^2\sin^2\theta = \xi^2$$

$$\xi_0 = \pm m\sin\theta \tag{5.32}$$

The point $\xi_0 = -m\sin\theta$ is the one of interest, as, the positive point would be used for consideration on the negative real axis in the range $-m \leq \xi_0 \leq 0$. Thus at the saddle point we obtain from $f(\xi) = i\xi\sin\theta - (\xi^2-m)^{1/2}\cos\theta$,

$$\begin{aligned} f(\xi_0) =& i(-m\sin\theta)\sin\theta - (m^2\sin^2\theta - m^2)^{1/2}\cos\theta, \\ =& -im\sin^2\theta - m(\sin^2\theta - 1)^{1/2}\cos\theta, \\ =& -im\sin^2\theta - m(-cos^2\theta)^{1/2}\cos\theta, \\ =& -im\sin^2\theta - -im\cos^2\theta, \\ =& -im. \end{aligned} \tag{5.33}$$

We also obtain

$$
\begin{aligned}
f''(\xi) =& -\frac{\cos\theta}{(\xi^2-m^2)^{1/2}} + \frac{\xi^2\cos\theta}{(\xi^2-m^2)^{3/2}},\\
f''(\xi_0) =& -\frac{\cos\theta}{(m^2\sin^2\theta-m^2)^{1/2}} + \frac{m^2\sin^2\theta\cos\theta}{(m^2\sin^2\theta-m^2)^{3/2}},\\
=& -\frac{\cos\theta}{(-m^2\cos^2\theta)^{1/2}} + \frac{m^2\sin^2\theta\cos\theta}{(-m^2\cos^2\theta)^{3/2}},\\
=& -\frac{\cos\theta}{im\cos\theta} + \frac{m^2\sin^2\theta\cos\theta}{-im^3\cos^3\theta},\\
=& -\frac{1}{im} - \frac{\sin^2\theta}{im\cos\theta} = \frac{i}{m} + \frac{i\sin^2\theta}{m\cos\theta},\\
=& \frac{im\cos^2\theta + im\sin^2\theta}{m\cos^2\theta},\\
=& \frac{i}{m\cos^2\theta},\\
=& \frac{i\sec^2\theta}{m}.
\end{aligned}
\tag{5.34}
$$

As before, along the deformed contour we may write $f(\xi) = f_1(\xi) + if_2(\xi_0)$ and as f_2 is constant we may write $f(\xi) = f_1(\xi) - u^2 = \frac{f''(\xi_0)(\xi-\xi_0)^2}{2}$. Now we can determine the shape of the deformed contour

$$
\begin{aligned}
-u^2 =& \frac{i\sec^2(\xi-\xi_0)^2}{2m},\\
-\frac{2mu^2}{i\sec^2\theta} =& (\xi-\xi_0)^2,\\
2imu^2\cos^2\theta =& (\xi-\xi_0)^2,\\
2e^{i\pi/2}mu^2\cos^2\theta =& (\xi-\xi_0)^2,\\
\pm\sqrt{2m}e^{i\pi/4}u\cos\theta =& \xi-\xi_0, && (5.35)\\
\xi(u) =& \pm\sqrt{2m}e^{i\pi/4}u\cos\theta + \xi_0, && (5.36)
\end{aligned}
$$

where the sign will be determined by the direction in which the contour passes. Notice also

$$\xi(0) = \xi_0 = -m\sin\theta, \tag{5.37}$$

and

$$\frac{d\xi}{du} = \pm\sqrt{2m}e^{i\pi/4}\cos\theta. \tag{5.38}$$

We need to determine the behaviour of the path away from the saddle points. The points where the path intersects the real ξ-axis are

$$\mathrm{Im}\,(f(\xi) - f(\xi_0)) = 0, \quad \xi \in \mathbb{R}.$$

Where the first condition is true for all points along our steepest descent path, and the second gives the points of real axis intersection. From here we can substitute (5.11) and (5.33) into the condition above gives $\xi_1 = -m\csc\theta$ as the only intersection point other than the branch point (the asymptotes also pass through this). From here we can find the asymptotic behaviour of the path. Now writing the above condition as Im $f(\xi) =$ Im $f(\xi_0)$ we see

$$\mathrm{Im}\left(i\xi\sin\theta - (\xi^2-m^2)^{1/2}\cos\theta\right) = -m.$$

Large $|\xi|$ will be dominant in the above condition, thus we neglect m, hence

$$\mathrm{Im}\,(i\sin\theta \mp \cos\theta) = -m.$$

Let $\xi = \zeta + i\eta$, we see the lines of the asymptotes are given by

$$\zeta \sin\theta \mp \eta\cos\theta = -m.$$

From here, based on the direction of passage we will select the positive sign. Now we are in a position to study the geometry of the deformed contour along the negative real axis relative to the pole $\xi = -\xi_R$, and two branch points $\xi = -1, -k$ and we have $1 < k < \xi_R$.

The deformed steepest-descent contour has added a “return loop” that returns from infinity and passes about the branch point in a proper manner, then returns off to infinity. This is necessary for the case when $\theta > \csc^{-1} k$, and thus $\xi_1 > -k$, because the portion that is negatively sloping is not properly circulating the branch point. So, the return loop is added to account for this $-k$. It is stated in Miller and Pursey [1954] that the contributions of these additional loops is asymptotically negligible. When $\xi_0 = -1$, and $m = -1$, there is no issue of the positive sloping portion of the path not properly passing about the branch point, Γ_α is made to coincide with the steepest-descent path.

It still remains to determine the path around the vicinity of the pole $-\xi_R$. When $\theta < \csc^{-1}(\xi_R/m)$, the cross over point ξ_1 is to the right of ξ_R, thus the pole is no longer inside the contour. However, when $\theta > \csc^{-1}(\xi_R/m)$, the pole is no inside the contour and is accounted for by the additional residue, which contains $e^{-R(\xi_R^2 - m^2)}\cos\theta$. We clearly see the contribution from this vanishes for large R and thus is neglected, as we search for approximate far field displacements. The Contribution of the poles for small R near the source is not negligible and will be a large source of error. When $\theta = \pi/2$, this is the case of surface waves, where the residue is the dominant term and cant be neglected for far field displacement. This will be considered later.

Now that the path has been properly determined we can return to (5.31); considering the first order expansion, and all appropriate substitutions from above, (Note that first order is a decent approximation as the error is of order $1/R^{1/2}$ which is very slow) we have

$$I_1 \sim \frac{d\xi}{du} e^{Rf(\xi_0)} \chi(0) \frac{\sqrt{\pi}}{R^{1/2}}, \tag{5.39}$$

$$\sim \sqrt{\frac{2\pi m}{R}} e^{Rf(\xi_0)} e^{i\pi/4} \cos\theta \chi(0), \tag{5.40}$$

$$I_1 \sim \sqrt{\frac{2\pi m}{R}} e^{i(\pi/4 - Rm)} \cos\theta \chi(-m\sin\theta). \tag{5.41}$$

Finally from here we are in a position to obtain the displacements. We have an expression for I_1 containing generalised terms $m = 1$, k and χ. We compare the integral I_1 to the original displacement equation (3.18) and see

$$\chi_1^{(x)}(\xi) = \frac{1}{i\mu\pi} \frac{\sin\xi a}{F_0(\xi)} (k^2 - 2\xi^2), \tag{5.42}$$

$$\chi_k^{(x)}(\xi) = \frac{1}{i\mu\pi} \frac{\sin\xi a}{F_0(\xi)} 2(\xi^2 - 1)^{1/2} (\xi^2 - k^2)^{1/2}, \tag{5.43}$$

for (3.19)

$$\chi_1^{(y)}(\xi) = \frac{1}{\mu\pi} \frac{(\xi^2 - 1)^{1/2} \sin\xi a}{\xi F_0(\xi)} (k^2 - 2\xi^2), \tag{5.44}$$

$$\chi_k^{(y)}(\xi) = \frac{1}{\mu\pi} \frac{(\xi^2 - 1)^{1/2} \sin\xi a}{\xi F_0(\xi)} 2\xi^2, \tag{5.45}$$

and for I_1

$$I_1 \sim \sqrt{\frac{2\pi}{R}} e^{i\pi/4} \cos\theta \left[\chi_1(-\sin\theta) e^{-iR} + \sqrt{k}\, \chi_k(-k\sin\theta) e^{-ikR} \right]. \tag{5.46}$$

Note that now we let $a \to 0$, but let the pressure remain constant. hence

$$u_x \sim \sqrt{\frac{2\pi}{R}} e^{i\pi/4} \cos\theta \left[\chi_1^{(x)}(-\sin\theta)e^{-iR} + \sqrt{k}\,\chi_k^{(x)}(-k\sin\theta)e^{-ikR}\right]. \tag{5.47}$$

$$u_y \sim \sqrt{\frac{2\pi}{R}} e^{i\pi/4} \cos\theta \left[\chi_1^{(y)}(-\sin\theta)e^{-iR} + \sqrt{k}\,\chi_k^{(y)}(-k\sin\theta)e^{-ikR}\right]. \tag{5.48}$$

Where we still need to convert to a curvilinear coordinate system (and Cartesian for plotting), and evaluate the χ functions. We will find u_R, u_θ for a more elegant solution before coming to interpreting the displacements. To this end we use the relations

$$u_R = u_y \cos\theta + u_x \sin\theta, \tag{5.49}$$

$$u_\theta = u_x \cos\theta - u_y \sin\theta. \tag{5.50}$$

or

$$\begin{bmatrix} u_R \\ u_\theta \end{bmatrix} = \begin{bmatrix} \sin\theta & \cos\theta \\ \cos\theta & -\sin\theta \end{bmatrix} \begin{bmatrix} u_x \\ u_y \end{bmatrix} \tag{5.51}$$

First however we need simplified versions of (5.47) and (5.48). Starting with (5.47)

$$u_x \sim \sqrt{\frac{2\pi}{R}} \frac{e^{i\pi/4}\cos\theta}{i\mu\pi} \left[e^{-iR} \frac{\sin(-a\sin\theta)(k^2 - 2\sin^2\theta)}{F_0(-\sin\theta)} \right. \\ \left. + e^{-ikR} \frac{\sqrt{k}\sin(-ka\sin\theta)2(k^2\sin^2\theta - 1)^{1/2}(k^2\sin^2\theta - k^2)^{1/2}}{F_0(-k\sin\theta)} \right]. \tag{5.52}$$

Notice $F_0(-m\sin\theta) = F_0(m\sin\theta)$, and

$$u_x \sim \sqrt{\frac{2}{R\pi}} \frac{e^{i\pi/4}\cos\theta}{\mu} \left[e^{-iR} \frac{i\sin(a\sin\theta)(k^2 - 2\sin^2\theta)}{F_0(\sin\theta)} \right. \\ \left. - e^{-ikR} \frac{k^{3/2}\sin(ka\sin\theta)2\cos\theta(k^2\sin^2\theta - 1)^{1/2}}{F_0(k\sin\theta)} \right]. \tag{5.53}$$

Now we can first order Taylor expand to get

$$u_x \sim \sqrt{\frac{2}{R\pi}} \frac{e^{i\pi/4}\cos\theta}{\mu} \left[e^{-iR} \frac{ia\sin\theta(k^2 - 2\sin^2\theta)}{F_0(\sin\theta)} - e^{-ikR} \frac{k^{5/2}a2\sin\theta\cos\theta(k^2\sin^2\theta - 1)^{1/2}}{F_0(k\sin\theta)} \right]. \tag{5.54}$$

Hence

$$u_x \sim \sqrt{\frac{2}{R\pi}} \frac{ae^{i\pi/4}\cos\theta}{\mu} \left[e^{-iR} \frac{i\sin\theta(k^2 - 2\sin^2\theta)}{F_0(\sin\theta)} - e^{-ikR} \frac{k^{5/2}\sin 2\theta(k^2\sin^2\theta - 1)^{1/2}}{F_0(k\sin\theta)} \right]. \tag{5.55}$$

Now for (5.48)

$$u_y \sim \sqrt{\frac{2\pi}{R}} \frac{e^{i\pi/4}\cos\theta}{\mu\pi} \left[\frac{(\sin^2\theta - 1)^{1/2}\sin(-a\sin\theta)}{-\sin\theta F_0(\sin\theta)}(k^2 - 2\sin^2\theta)e^{-iR} \right. \\ \left. + \sqrt{k}\frac{(k^2\sin^2\theta - 1)^{1/2}\sin(-ak\sin\theta)}{-k\sin\theta F_0(k\sin\theta)} 2k^2\sin^2\theta e^{-ikR} \right], \tag{5.56}$$

$$u_y \sim \sqrt{\frac{2}{R\pi}} \frac{e^{i\pi/4}\cos\theta}{\mu} \left[\frac{(\sin^2\theta - 1)^{1/2}\sin(a\sin\theta)}{\sin\theta F_0(\sin\theta)}(k^2 - 2\sin^2\theta)e^{-iR} \right. \\ \left. + \frac{(k^2\sin^2\theta - 1)^{1/2}\sin(ak\sin\theta)}{k\sin\theta F_0(k\sin\theta)} 2k^{5/2}\sin^2\theta e^{-ikR} \right], \tag{5.57}$$

$$
u_y \sim \sqrt{\frac{2}{R\pi}}\frac{ae^{i\pi/4}\cos\theta}{\mu}\left[\frac{(\sin^2\theta-1)^{1/2}\sin\theta}{\sin\theta F_0(\sin\theta)}(k^2-2\sin^2\theta)e^{-iR}\right.
$$

$$
\left. + \frac{(k^2\sin^2\theta-1)^{1/2}k\sin\theta}{k\sin\theta F_0(k\sin\theta)}2k^{5/2}\sin^2\theta e^{-ikR}\right], \tag{5.58}
$$

$$
u_y \sim \sqrt{\frac{2}{R\pi}}\frac{ae^{i\pi/4}\cos\theta}{\mu}\left[\frac{i\cos\theta(k^2-2\sin^2\theta)}{F_0(\sin\theta)}e^{-iR} + \frac{(k^2\sin^2\theta-1)^{1/2}2k^{5/2}\sin^2\theta}{F_0(k\sin\theta)}e^{-ikR}\right]. \tag{5.59}
$$

Now using (5.49), (5.55), and (5.59) we get

$$
u_R \sim \sqrt{\frac{2}{R\pi}}\frac{ae^{i\pi/4}\cos^2\theta}{\mu}\left[\frac{i\cos\theta(k^2-2\sin^2\theta)}{F_0(\sin\theta)}e^{-iR} + \frac{(k^2\sin^2\theta-1)^{1/2}2k^{5/2}\sin^2\theta}{F_0(k\sin\theta)}e^{-ikR}\right]
$$

$$
+ \sqrt{\frac{2}{R\pi}}\frac{ae^{i\pi/4}\sin\theta\cos\theta}{\mu}\left[e^{-iR}\frac{i\sin\theta(k^2-2\sin^2\theta)}{F_0(\sin\theta)} - e^{-ikR}\frac{k^{5/2}\sin 2\theta(k^2\sin^2\theta-1)^{1/2}}{F_0(k\sin\theta)}\right]. \tag{5.60}
$$

Continuing on

$$
u_R \sim \sqrt{\frac{2}{R\pi}}\frac{ae^{i\pi/4}\cos\theta}{\mu}\left[\frac{i\cancel{\cos^2\theta}(k^2-2\sin^2\theta)}{F_0(\sin\theta)}e^{-iR} + \cancel{\frac{(k^2\sin^2\theta-1)^{1/2}2k^{5/2}\sin^2\theta\cos\theta}{F_0(k\sin\theta)}e^{-ikR}}\right.
$$

$$
\left. \cancel{+ e^{-iR}\frac{i\sin^2\theta(k^2-2\sin^2\theta)}{F_0(\sin\theta)}} - \cancel{e^{-ikR}\frac{k^{5/2}\sin\theta\sin 2\theta(k^2\sin^2\theta-1)^{1/2}}{F_0(k\sin\theta)}}\right]. \tag{5.61}
$$

Considering the standard trigonometric identities we see the cancellations above, and can simplify this to

$$
u_R \sim \sqrt{\frac{2}{R\pi}}\frac{ae^{i\pi/4}\cos\theta}{\mu}\frac{i(k^2-2\sin^2\theta)}{F_0(\sin\theta)}e^{-iR}, \tag{5.62}
$$

$$
u_R \sim \sqrt{\frac{2}{R\pi}}\frac{iae^{i\pi/4}e^{-iR}\cos\theta(k^2-2\sin^2\theta)}{\mu F_0(\sin\theta)}, \tag{5.63}
$$

$$
u_R \sim \sqrt{\frac{2}{R\pi}}\frac{ae^{i(3\pi/4-R)}\cos\theta(k^2-2\sin^2\theta)}{\mu F_0(\sin\theta)}, \tag{5.64}
$$

which is our final radial displacement. Considering now (5.50), (5.55), and (5.59) we see

$$
u_\theta \sim \sqrt{\frac{2}{R\pi}}\frac{ae^{i\pi/4}\cos^2\theta}{\mu}\left[e^{-iR}\frac{i\sin\theta(k^2-2\sin^2\theta)}{F_0(\sin\theta)} - e^{-ikR}\frac{k^{5/2}\sin 2\theta(k^2\sin^2\theta-1)^{1/2}}{F_0(k\sin\theta)}\right]
$$

$$
- \sqrt{\frac{2}{R\pi}}\frac{ae^{i\pi/4}\cos\theta\sin\theta}{\mu}\left[\frac{i\cos\theta(k^2-2\sin^2\theta)}{F_0(\sin\theta)}e^{-iR} + \frac{(k^2\sin^2\theta-1)^{1/2}2k^{5/2}\sin^2\theta}{F_0(k\sin\theta)}e^{-ikR}\right]. \tag{5.65}
$$

Hence

$$
u_\theta \sim \sqrt{\frac{2}{R\pi}}\frac{ae^{i\pi/4}}{\mu}\left[\cancel{e^{-iR}\frac{i\sin\theta\cos^2\theta(k^2-2\sin^2\theta)}{F_0(\sin\theta)}} - \cancel{\frac{i\sin\theta\cos^2\theta(k^2-2\sin^2\theta)}{F_0(\sin\theta)}e^{-iR}}\right.
$$

$$
\left. - e^{-ikR}\frac{k^{5/2}\cancel{\cos^2\theta}\sin 2\theta(k^2\sin^2\theta-1)^{1/2}}{F_0(k\sin\theta)} - \cancel{\frac{(k^2\sin^2\theta-1)^{1/2}2k^{5/2}\sin^2\theta\cos\theta\sin\theta}{F_0(k\sin\theta)}}e^{-ikR}\right]. \tag{5.66}
$$

Using the same trigonometric identities as before. Now we can write

$$
u_\theta \sim -\sqrt{\frac{2}{R\pi}}\frac{ae^{i\pi/4}}{\mu}e^{-ikR}\frac{k^{5/2}\sin 2\theta(k^2\sin^2\theta-1)^{1/2}}{F_0(k\sin\theta)}, \tag{5.67}
$$

$$u_\theta \sim -\sqrt{\frac{2k^5}{R\pi}} \frac{ae^{i(\pi/4-kR)}\sin 2\theta(k^2\sin^2\theta-1)^{1/2}}{\mu F_0(k\sin\theta)}, \tag{5.68}$$

$$u_\theta \sim \sqrt{\frac{2k^5}{R\pi}} \frac{ae^{i(5\pi/4-kR)}\sin 2\theta(k^2\sin^2\theta-1)^{1/2}}{\mu F_0(k\sin\theta)}. \tag{5.69}$$

Where

$$F_0(-m\sin\theta) = (2m^2\sin^2\theta - k^2)^2 - 4m^2\sin^2\theta(m^2\sin^2\theta-1)^{1/2}(m^2\sin^2\theta-k^2)^{1/2}. \tag{5.70}$$

And hence we have obtained a final result for internal displacement fields in polar coordinates. The special case of surface waves will be considered later. But note, this arises when $y = 0$ or $\theta = \pi/2$ and the major contribution will be from the poles which have been neglected here.

6 Examining Internal Displacement Fields.

From the above results we can specify in desired parameters for k, μ and a, then obtain plots for the displacements. There are a number of ways to do this, here I will use maple to obtain 2-dimensional contour plots at some fixed R, then also 3-dimensional plots. This can either be done staying in polar coordinates or by shifting back to Cartesian. Note that all plots are of the real parts of the displacement fields.

First, to obtain a result similar to Graff [1991] we consider U_R, U_θ at a given R. For our parameters I will use: $a = 1, k = 2, \mu = 1$, and $0 \le \theta < \pi/2$.

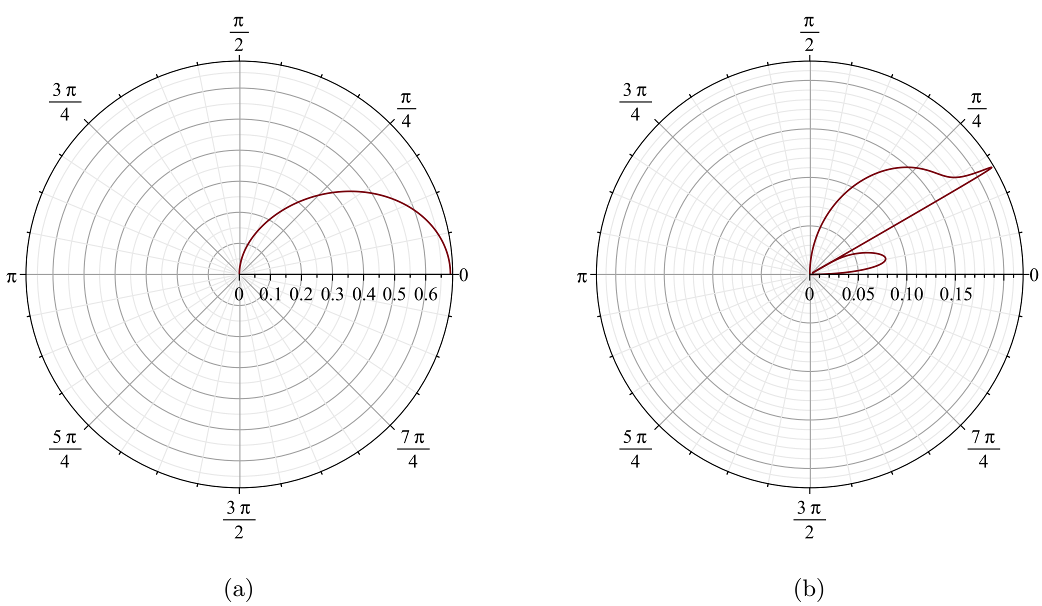

Figure 1: Displacement (a) u_R ($R = 1$) and (b) u_θ ($R = 2.02$)

In Graff [1991] [pp. 352] it isn't specified exactly what parameters are used but as we can see the polar plots of figure 1 are very similar. In Miller and Pursey [1954] they provide more details on the parameters used. The surface corresponds to the line going vertically down through the origin, and the forcing would correspond to the point at the origin perpendicular to this line, and forcing to the right. In U_θ two distinct lobes are visible this is caused by zeros in the numerator.

For a more intuitive visualisation it is better to switch to Cartesian and plot in 3-dimensions. To this end we make the substitutions $R = \sqrt{x^2+y^2}$, $\cos\theta = y/\sqrt{x^2+y^2}$, $\sin\theta = x/\sqrt{x^2+y^2}$, and $\sin 2\theta = 2xy/(x^2+y^2)$ to (4.55), (4.59). This is shown in figure 2.

However, for the best visualisation we need to plot the magnitude of the real parts of u_x and u_y, this will give us a very good idea of what is happening. This is done in figure 3 where we have plotted Re $(u_x^2 + u_y^2)$. We can clearly see the nature of the load as well as the wave decay. We also note again that we used asymptotic approximations at infinity, and thus we shouldn't expect this solution to be particularly accurate near the source as the poles have been neglected. Thus, we don't see certain features that we would expect to see in reality, such as, surface waves, shear windows (regions of significant shear waves), and pressure waves. However, the far field accuracy we expect to be good. More analysis will be considered after the finite element analysis. Note that figure 2 and figure 3 have non constrained scaling of the coordinate axis.

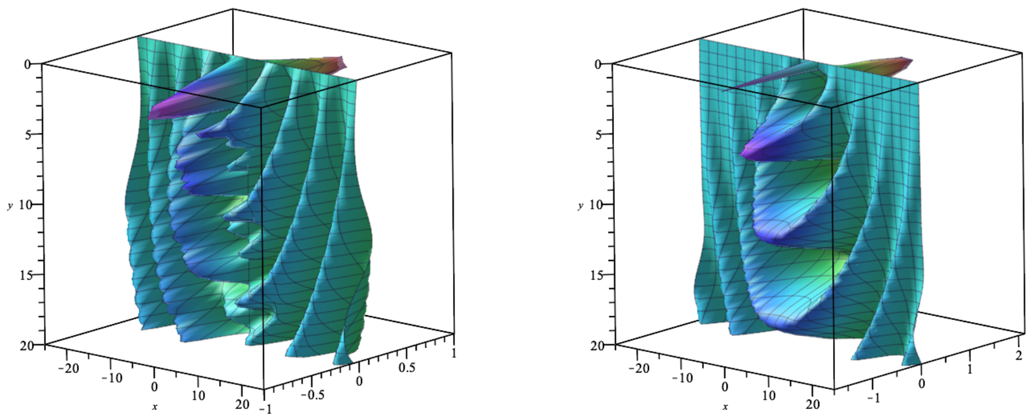

(a) (b)

Figure 2: Displacement (a) u_x and (b) u_y

Figure 3 is presented on the following page.

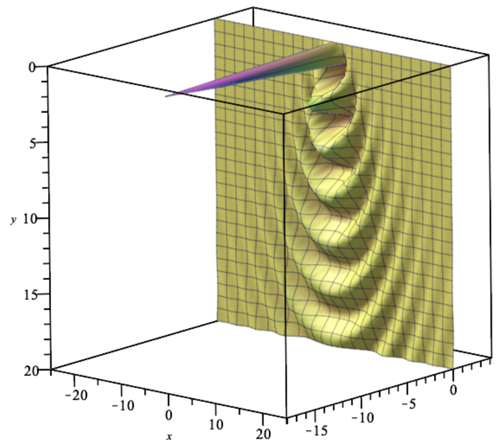

Figure 3: Combined displacement magnitude

7 Surface Waves.

The special case of surface waves arise when $\theta = \pi/2$ or $y = 0$. Intuitively these both imply we are on the surface. Considering (3.18), (3.19) for $y = 0$ we have the displacements

$$u_x(x,0) = \frac{1}{i\mu\pi}\int_{-\infty}^{\infty}\frac{\xi a}{F_0(\xi)}\left[2(\xi^2-1)^{1/2}(\xi^2-k^2)^{1/2}+(k^2-2\xi^2)\right]e^{i\xi x}d\xi, \tag{7.1}$$

$$u_y(x,0) = \frac{1}{\mu\pi}\int_{-\infty}^{\infty}\frac{(\xi^2-1)^{1/2}a}{F_0(\xi)}k^2 e^{i\xi x}d\xi, \tag{7.2}$$

where the $\sin\xi a$ terms have been dealt with via Taylor expansion as we have the limit $a \to 0$, but recall we let the pressure remain constant. Simplifying this to get

$$u_x(x,0) = \frac{a}{i\mu\pi}\int_{-\infty}^{\infty}\frac{\xi}{F_0(\xi)}\left[2(\xi^2-1)^{1/2}(\xi^2-k^2)^{1/2}+(k^2-2\xi^2)\right]e^{i\xi x}d\xi, \tag{7.3}$$

$$u_y(x,0) = \frac{ak^2}{\mu\pi}\int_{-\infty}^{\infty}\frac{(\xi^2-1)^{1/2}}{F_0(\xi)}e^{i\xi x}d\xi. \tag{7.4}$$

We perform the same contour integration as before but now we only consider contribution from the poles and contribution from the branch cuts is ignored, and we reiterate this is because we see in the residues of the poles a factor of $e^{-Rg\cos\theta}$ where $g = g(\xi_R, m)$. Thus in the limit problem of $R \to \infty$ this term is negligible, apart from the case when $\theta = \pi/2$ where it is in fact the dominant term. Hence, in the limit problem (the far field), contribution from the branch cut integrals specifically corresponds to the interior waves and not the surface waves. If we were to inspect the limit problem of interior waves near the source we would expect to see significant error as we have R small and thus we are missing contribution from the poles. Moving on, we see these integrands are in the form

$$\Omega(\xi) = \frac{\psi(\xi)}{F_0(\xi)}, \tag{7.5}$$

and we have the poles $\pm\xi_R$. We use only the negative pole as we require the decay condition of the wave, as by convention the negative pole represents waves originating from the origin and the positive represents waves coming from infinity, which the latter we regard in this situation as nonphysical. We have the following for the residue of quotients $f(z) = g(z)/h(z)$ where c is a pole

$$\mathrm{Res}(f,c) = \lim_{z\to c}(z-c)f(z) = \lim_{z\to c}\frac{zg(z)-cg(z)}{h(z)}, \tag{7.6}$$

apply L'Hôpital,

$$= \lim_{z\to c}\frac{g(z)+zg'(z)-cg'(z)}{h'(z)} = \frac{g(c)}{h'(c)}. \tag{7.7}$$

Hence we have

$$\mathrm{Res}(\Omega,-\xi_R) = \frac{\psi(-\xi_R)}{F_0'(-\xi_R)}. \tag{7.8}$$

Using Cauchy's residue theorem we get

$$\oint_\gamma f(z)dz = 2\pi i\sum_k \mathrm{Res}(f,c_k). \tag{7.9}$$

For u_x we have

$$u_x(x,0) = -\frac{2a\xi_R e^{-i\xi_R x}}{\mu F_0'(-\xi_R)}\left[2(\xi_R^2-1)^{1/2}(\xi_R^2-k^2)^{1/2}+(k^2-2\xi_R^2)\right], \tag{7.10}$$

and for u_y

$$u_y(x,0) = \frac{2iak^2(\xi_R^2-1)^{1/2}}{\mu F_0'(-\xi_R)}e^{-i\xi_R x}. \tag{7.11}$$

From here we specify desired constants values (here: $a=1, k=2, \mu=1, \xi_R=-2.144712535$) and get the plots figure 4 and figure 5.

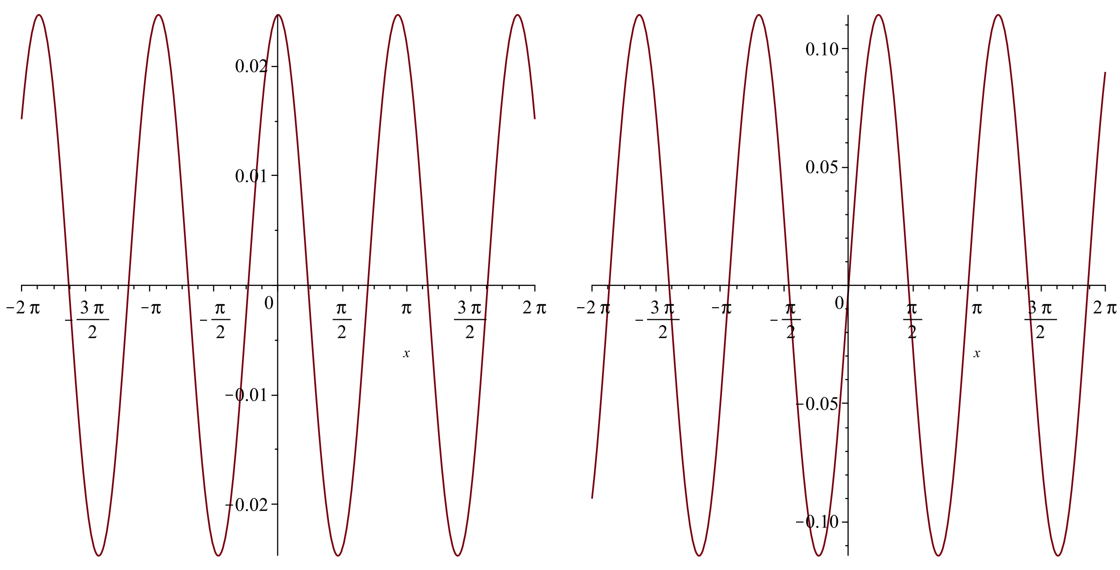

(a) (b)

Figure 4: Displacement in (a) x and (b) y directions on the surface

The first thing to note about these plots is that they do not decay as they move further away from the origin, whereas the bulk waves decay as $R^{-1/2}$. This is a consequence of the source being an line-load of plain-strain, if the source were a point load then the surface waves would also decay with but not as severely as the bulk waves into the interior.

The second thing to note is that the displacement in x is much smaller than the displacement in y and there is a difference in phasing. This is because the trajectory of a point on the surface is that of an ellipse, retrograde to the direction of wave propagation, with the major axis lined up in the y direction and the minor axis lined up with the x direction.

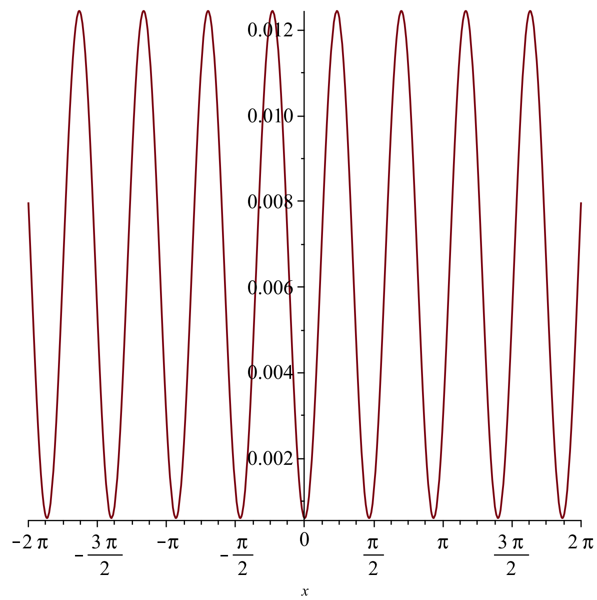

Figure 5: Combined displacement magnitude

In figure 5 we have plotted Re $(u_x^2 + u_y^2)$ for surface waves.

8 Finite Element Numerical Analysis.

In this section I will compare the results I obtained for far field displacements with asymptotic methods with that of finite element numerical analysis done in COMSOL Multiphysics.

We begin by setting up the problem; we create a finite 2-dimensional rectangular domain and add a point source to the surface. For the point source we specify it be of unit magnitude time-harmonic normal loading. For the boundary's we have several options for the bottom and sides of the domain but it is critical the surface boundary be left free. For the bottom and sides the best option is to expand the domain and use perfectly matched layers (PML) figure 8 and figure 9. These are artificial absorbing layers which simulate the condition of an open domain. (PML) are designed such that waves do not reflect on the interface; this is important as reflected waves inside are finite domain will compromise our results. Another option for the boundary conditions on the sides and bottom is using a low reflecting boundary figure 6 and figure 7. These aim to archive the same thing as (PML) but are less effective. We also specify zero initial values for the internal displacement fields, and set the material parameters of a linearly elastic isotropic solid such that they are in accordance with what we have used in our previous plots for interior waves and surface waves. We set an extremely fine mesh, this is important in the accuracy and stability of our results. A coarse mesh is computationally less expensive but lacks the required stability and accuracy of a fine mesh. We also note that an adaptive mesh could be use to get the best of both, where regions of rapidly changing displacement have a fine mesh and regions of slowing changing displacement have a coarser mesh. We then solve the resulting problem in the frequency domain, specifying a desired frequency such that we get clearly defined waves in the finite domain.

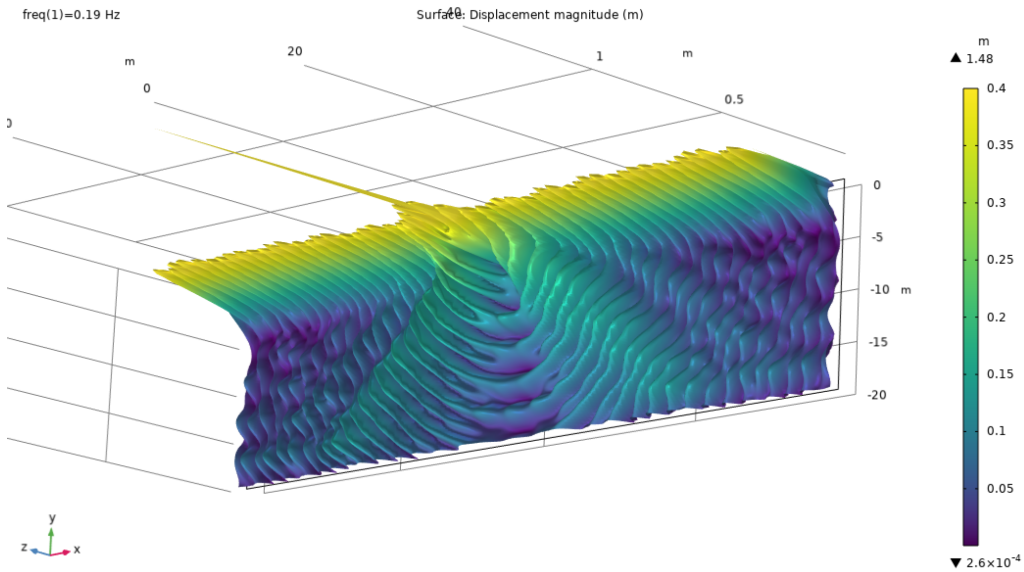

Figure 6: Displacement field

Figure 6 and figure 7 are the results obtained from COMSOL multiphysics. We see a large displacement directly at the source similar to our asymptotic plots. However, in figure 6 and figure 7 we see waves propagating along the surface this differs from the asymptotic plot figure 3. This is because we omitted contribution from the poles which lead to surface waves and considered them separately. We also see the waves going downwards from the source in a similar fashion to figure 3, but with notable differences in shape. In figure 6 and figure 7 we observe shear windows, like an inverted "v" directly below the source. These are regions of significant shear waves. Waves present above and blow these shear windows result from pressure waves, which disperse in a semi-circular fashion originating from the source. However, we do notice figure 6 and 7 are not smooth like figure 3 and this is because we have use low reflecting boundaries, which have reflected waves back into the finite domain from the interface. We observe that using a (PML) in figure 8 and 9 has alleviated this.

In figure 8a we have a plot where we have tripled the height of the domain, adjusted the frequency to 1.2Hz (so the waves are more defined in this larger domain) and added PML. We see very similar structures in figure 8 to those in figure 6 and figure 7 (surface waves, shear windows, pressure waves) and we should also note here (as it is more obvious) we see the wave number directly below the source has decreased as the waves are combining but, on the edges of the "v", they are still distinct. This is again a result from the shear window and pressure waves interacting. We also note here that the amplitudes of displacement are greatest on the surface, then in the shear windows, then finally lowest in the pressure wave dominated regions. This is because, the percentage of total energy each of these wave types gets is (as it is quoted in Graff [1991] [pp. 356]) surface waves (Rayleigh waves) receive 67% of the energy, shear waves receive 26% of the energy and finally pressure waves receive 7% of the energy.

In figure 8b we have now considered the case of a line load (of length 5) on the boundary with the same increased domain and PML as figure 8a, but with the frequency at 1.9Hz. We have done this to illustrate that in elasticity, point sources create singular stress fields. Here there still are singularities at the endpoints of the line. For the formal asymptotic case we use a regularisation procedure, where we start with a finite source and then let the width of this strip go to zero and thus don't have a singular field. We could also weight the excitation so that it vanishes, smoothly, at the end points (-2.5,2.5) (figure 9).

In figure 9 we have the same problem as before but we have set the force acting on the line to be

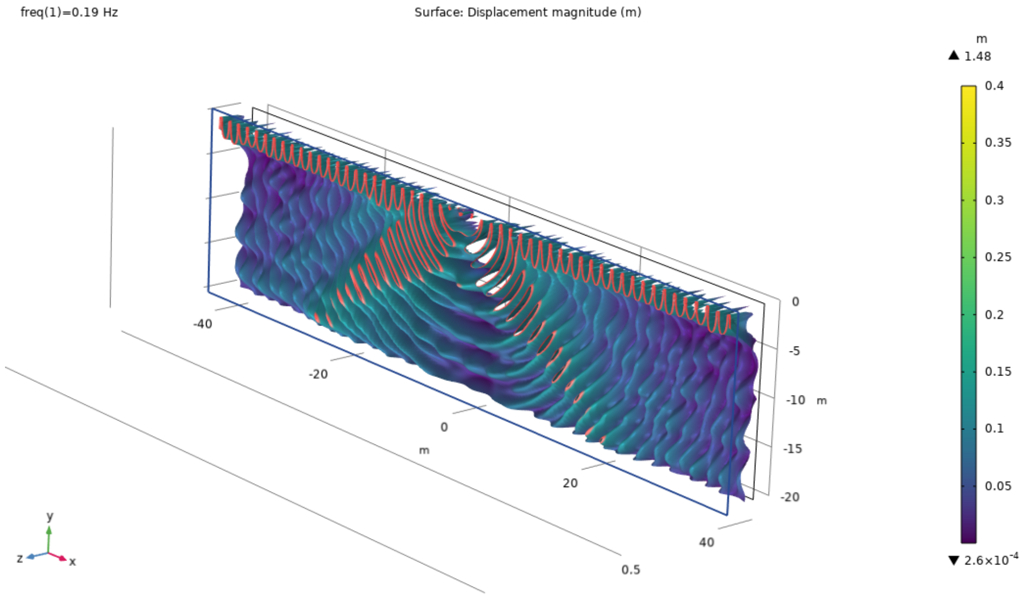

Figure 7: Displacement field with intersection plane

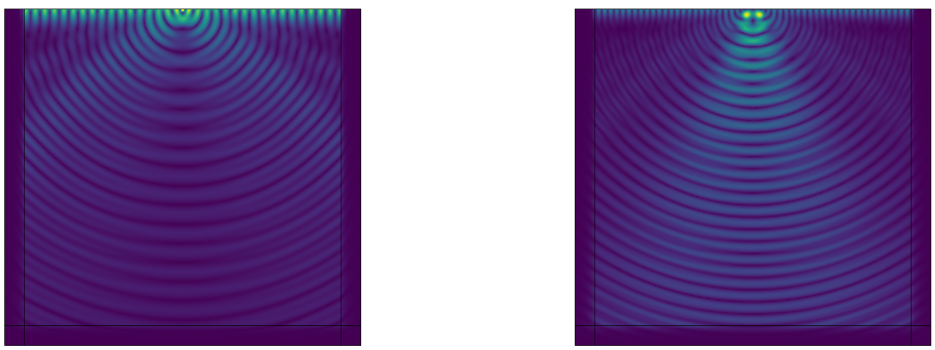

(a)

(b)

Figure 8: (a) Displacement field with point source and PML. (b) Displacement field with Line source and PML

$-(|x|-2.5)^2$. i.e., we have set the excitation such that it vanishes, smoothly, at the end points (-2.5,2.5). Now we have a non singular displacement field, but not of unity force.

In figure 6, figure 7, figure 8, and figure 9 we see very similar surface waves. And these are in fact similar to the surfaces waves obtained in our previous analysis in figure 4 and figure 5. This further indicates that neglecting contribution from the branch cut integrals for the case of surface didn't appear to effect the results to a great extent. This is what we were expect as the contribution from the poles should be the dominant term.

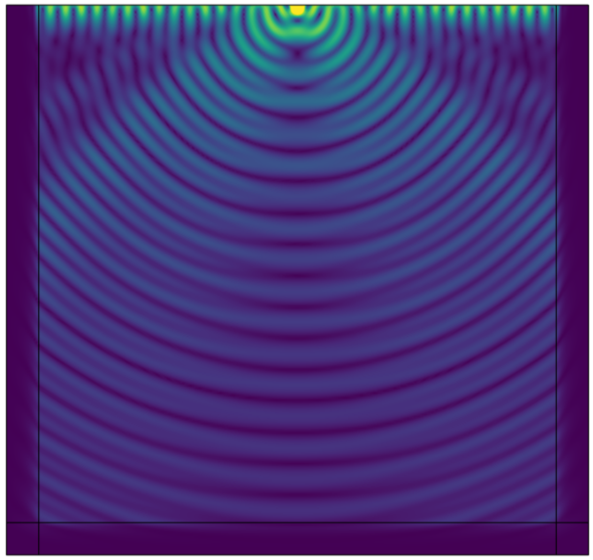

Figure 9: Displacement field with Smoothly vanishing line source and PML

9 Concluding Remarks.

We reiterate that the asymptotic method used here gives an approximate solution for far field displacements and hence decreased accuracy at the source as we have seen in our analysis and comparison to a finite element method. Asymptotic methods are still useful for the cases where we would like to check Finite element simulations, and ensure we are getting results in accordance with what we would expect. Or, situations where a finite element method maybe inapplicable.

To briefly summarise our work we first derived four conditions; the displacement equations, the wave equations, the stresses, and the boundary conditions. We then applied Fourier transforms to these results in the spacial variable x so that we could solve the system in a Fourier system of coordinates. Subsequently, we applied the inverse Fourier transform to obtain exact solutions in terms of definite integrals. This left us to consider the case of surface waves and interior waves separately, where we neglected contribution from the branch cut integrals and poles respectively. For the case of the branch cut integrals we performed the method of steepest descent, where we used a coordinate transformation to deformed the contour of integration such that it would pass through saddle points. Then, in this form we could asymptotically approximate the integrals and obtain solutions for far field interior displacements. Now considering the case of the poles and thus surface waves, we neglected contribution from the branch cut integrals and used Cauchy's residue theorem to obtain displacements on the surface. Next, we used a finite element numerical method to approximate the problem in a finite domain, but using perfectly matched layers (PML) to simulate our open domain. Finally, we performed a qualitative comparison between the asymptotic and finite element methods noting key differences, especially in the near source regime where we would expect large errors in the asymptotic method.

For further analysis it would be interesting and informative to conduct a quantitative comparison between finite element and asymptotic methods and compare not only near source results but far field results. One could also construct a higher order asymptotic approximation and again compare to see if this would improve things. Similar problems of dispersion of waves in layered mediums, as well as, problems of buried sources could be attacked in a similar fashion to what we have done here. Another potentially interesting problem to consider would be dispersion of waves in an elastic half spaces with the presence of a void (or many voids) in the solid. Time-harmonic forces could also be replaced by transient forces in this problem or any of the above problems.

Nonetheless, it is still impressive what can be done by hand in such complex problems, and to see it be of use in many areas like seismology, engineering, seismic prospecting, as well as others. However, the power of a modern finite element numerical method should not go unrecognised. There are of course many limitations and caveats (such as computational expense, errors associated with complex geometry, round off errors, etc.), but the ease at solving very complex problems which not so long ago was thought perhaps unachievable is indeed remarkable.

References

Jan Achenbach. *Wave propagation in elastic solids.* Elsevier, 2012.

ET Copson. Harold jeffreys, asymptotic approximations (clarendon press: Oxford university press, 1962), 144 pp., 30s. *Proceedings of the Edinburgh Mathematical Society*, 13(2):194–195, 1962.

William Maurice Ewing, Wenceslas S Jardetzky, Frank Press, and Arthur Beiser. Elastic waves in layered media. *Physics Today*, 10(12):27, 1957.

Karl F Graff. *Wave motion in elastic solids.* Dover, 1991.

Patrick Aidan Heelan. On the theory of head waves. *Geophysics*, 18(3):871–893, 1953a.

Patrick Aidan Heelan. Radiation from a cylindrical source of finite length. *Geophysics*, 18(3):685–696, 1953b.

Harold Jeffreys. On compressional waves in two superposed layers. *Mathematical Proceedings of the Cambridge Philosophical Society*, 23(4):472–481, 1926.

Horace Lamb. I. on the propagation of tremors over the surface of an elastic solid. *Philosophical Transactions of the Royal Society of London. Series A, Containing papers of a mathematical or physical character*, 203 (359-371):1–42, 1904.

Ernest Ralph Lapwood. The disturbance due to a line source in a semi-infinite elastic medium. *Philosophical Transactions of the Royal Society of London. Series A, Mathematical and Physical Sciences*, 242(841): 63–100, 1949.

GF Miller and H Pursey. The field and radiation impedance of mechanical radiators on the free surface of a semi-infinite isotropic solid. *Proceedings of the Royal Society of London. Series A. Mathematical and Physical Sciences*, 223(1155):521–541, 1954.

Morris Muskat. The theory of refraction shooting. *Physics*, 4(1):14–28, 1933.

Hiroshi Nakano. On rayleigh wave. *Japanese Journal of Astronomy and Geophysics*, 2(234–326):27, 1925.

Margery Newlands. The disturbance due to a line source in a semi-infinite elastic medium with a single surface layer. *Philosophical Transactions of the Royal Society of London. Series A, Mathematical and Physical Sciences*, 245(896):213–308, 1952.

H Takeuchi and N Kobayashi. Wave generations from line sources within the ground. *Journal of Physics of the Earth*, 3(1):7–15, 1955.